AD-A173 885 LOW-FREQUENCY SHALLOW WATER ACOUSTICS (20 TO 500 HZ) 1/2
(U) WASHINGTON UNIV SEATTLE APPLIED PHYSICS LAB
M SCHULKIN ET AL MAY 86 APL-UW-8606 N00014-84-K-0646
UNCLASSIFIED F/G 20/1 NL

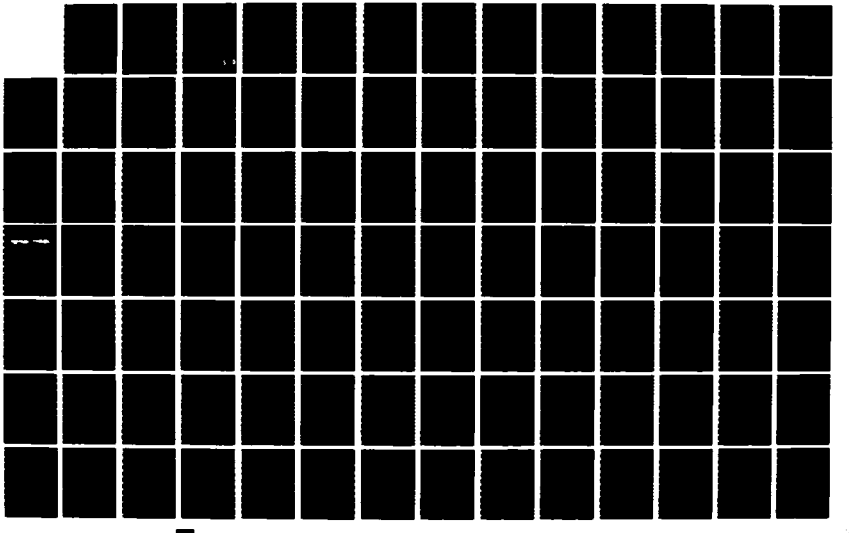

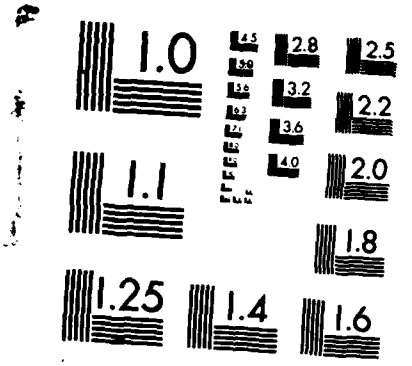

Low-Frequency Shallow Water Acoustics (20 to 500 Hz)

APL-UW 8606
May 1986

Approved for Public Release; Distribution is Unlimited

Contract N00014-84-K-0646 Mod 1

Low-Frequency Shallow Water Acoustics (20 to 500 Hz)

by
M. Schulkin
J.A. Mercer

APL-UW 8606
May 1986

Applied Physics Laboratory University of Washington
Seattle, Washington 98105

Approved for Public Release; Distribution is Unlimited

Contract N00014-84-K-0646 Mod 1

ACKNOWLEDGMENTS

The authors express their gratitude to Drs. T. Yamamoto (U. of Miami), G.V. Frisk (WHOI), F. Ingenito (NRL), W.A. Kuperman (NRL), S.N. Wolf (NRL), R.H. Bennett (NORDA), and S.O. McConnell (APL-UW) for their technical assistance in the preparation of this document and to Dr. S.R. Murphy for his support in having the document published. Dr. Murphy's incisive review and suggestions have improved the clarity of the document considerably. Encouragement and support were also provided by Drs. R.M. Fitzgerald (Code 425 UA) and J. H. Kravitz (Code 425 GG) of the Office of Naval Research under contract no. N00014-84-K-0646 Mod 1.

We also wish to thank the following for permission to reprint figures and tables from their published works: T. Akal, J.H. Beebe, T.M. Brocher, T.L. Foreman, E.L. Hamilton, B.T. Iwatake, F.B. Jensen, T.-K. Kan, W.A. Kuperman, D.A. Lindwall, S.T. McDaniel, H.J. McLellan, L.A. Rubano, R.D. Stoll, P.J. Vidmar, and T. Yamamoto.

ABSTRACT

The parameters affecting shallow water acoustic behavior at low frequencies (20 to 500 Hz) have been reviewed and an assessment has been made of their relative importance. The depth dependence of the sediment parameters, and stratigraphic layering, form the basis of geoacoustic models for which the wave equation may be solved. It is found that there is no unique approach to geoacoustic modeling. Typically, the additional information required includes *in situ* refraction, dispersion, and reflection measurements. Application of the Biot theory of sediment acoustics, which uses poroviscous parameters, leads to different conclusions in the frequency range of interest from those calculated using standard viscoelastic parameters alone. The Biot acoustic theory also explains successful data fits to semiempirical compressional and shear wave results. The most important sediment property is the flow permeability, which is equal to the choice of acoustic frequency in its effect. Its range of variability is so large that it is necessary to make a specific *in situ* determination of its magnitude for use in modeling and prediction. The permeability controls the relaxation frequency of the sediment and thus the rate of attenuation of both compressional and shear waves, their frequency dependence, and their velocity dispersion. Next in importance and requiring similar attention are the shear properties of the sediments, their related interface waves, and the skeletal frame loss. It is concluded that determination of these parameters *in situ* and further study in the laboratory are most important for progress.

TABLE OF CONTENTS

LIST OF FIGURES

LIST OF TABLES

PREFACE

The purpose of this study is to develop a procedure for isolating and quantifying the effects of the mechanisms that control the propagation of low frequency (20 to 500 Hz) acoustic signals in shallow water (20 to 200 m). A vast effort is in progress in this field and a large body of literature has been published. Workers from many different scientific and technical fields and geographic localities are converging in their efforts to describe mutual knowledge, concepts, and problems.

In addition to works in refereed journals, there are a number of books that contain a major source of information on bottom interactions and low frequency shallow water acoustics that are referenced at the end of the preface. The literature in the field of shallow water acoustics is so voluminous, extensive, repetitive, and overlapping in subject matter that our citations have been representative rather than complete. Many omissions have not been deliberate and probably will be found in the references that we cite. An extensive review of this literature has helped us to focus on the important mechanisms, their descriptive parameters, and issues yet to be resolved. Experimental procedures for isolating and quantifying mechanisms are usually interpreted in terms of laterally homogeneous sedimentary bottoms and start with geoacoustic models based on archival data for sediment properties and stratigraphy.

We omit the effects of sloping bottoms and rough boundary scattering in this report and concentrate on laterally homogeneous layers, since the problem of defining the critical elements of geoacoustic models appears to be most urgent at present.

General References

Conferences and Symposia

Physics of Sound in Marine Sediments, L. Hampton, Ed. (Plenum Press, New York, 1974).

Bottom-Interacting Ocean Acoustics, W.A. Kuperman and F.B. Jensen, Eds. (Plenum Press, New York, 1980).

Acoustics and the Sea-Bed: Conference Proceedings, N.G. Pace, Ed. (Bath University Press, Bath, UK, 1983).

Ocean Seismo-Acoustics — Low Frequency Underwater Acoustics, T. Akal and J.M. Berkson, Eds. (Plenum Press, New York, 1986).

Chapters in Books

Fundamentals of Ocean Acoustics, L.M. Brekhovskikh and Yu. Lysanov (Springer-Verlag, New York, 1982). Chapter 5: Propagation of sound in shallow water.

Waves in Layered Media, L.M. Brekhovskikh (Academic Press, New York, 1960). Chapter V: Wave propagation in layers; Chapter VI: The field of a concentrated source in a layered-inhomogeneous medium.

Propagation of Sound in the Ocean, M. Ewing, J.L. Worzel, and C.L. Pekeris (The Geological Society of America, Memoir 27, Boulder, Colorado, 1948). Theory of propagation of explosive sound in shallow water, by C.L. Pekeris.

Cavitation and Inhomogeneities in Underwater Acoustics: Proceedings of the First International Conference, Gottingen, Fed. Republic of Germany, 9-11 July 1979,W. Lauterborn, Ed. (Springer-Verlag, New York, 1980). On the influence of stochastic sound speed variations on acoustic transmission loss in shallow water, pp. 308-314, by H.G. Schneider.

Introduction to the Theory of Sound Transmission with Application to the Ocean, C.B. Officer (McGraw-Hill, New York, 1958). Chapter 3: Transmission in shallow water.

Ocean Acoustics, J.A. DeSanto, Ed. (Springer-Verlag, New York, 1979). Chapter 3: Numerical models of underwater acoustic propagation, by F.R. DiNapoli and R.L. Deavenport; Chapter 6: Inverse methods for reflector mapping and sound speed profiling, by N. Bleistein and J.K. Cohen.

Ocean Acoustics; theory and experiment in underwater sound, Ivan Tolstoy and C.S. Clay (McGraw-Hill, New York, 1966). Chapter 4: Propagation of sound in shallow water.

GLOSSARY OF TERMS[a]

A_r/A_i	amplitude reflection coefficient	p. 65
a	pore size parameter	p. 48
a_1	pore size parameter	p. 39
$a_{p\lambda}$	compressional wave attenuation, decibels per wavelength	p. 22
$a_{s\lambda}$	shear wave attenuation, decibels per wavelength	p. 22
a_p	compressional wave attenuation, dB/m	p. 16
a_s	shear wave attenuation, dB/m	p. 21
B	specific permeability, m^2 (or cm^2)	p. 5
b	angular attenuation rate, decibels/radian	p. 82
C_b	sound speed in seabed (bottom), m/s	p. 77
C_s	shear speed, m/s	p. 77
C_w	sound speed in water at bottom, m/s	p. 77
C_0	sound speed in water and subbottom, m/s	p. 62
C_1	sound speed in water at bottom, m/s	p. 82
C_2	sound speed in bottom, m/s	p. 83
D	depth in bottom, m	p. 13
d_{10}	diameter of grains at which 10% of soil is finer, mm	p. 30
d	mean grain diameter, mm	p. 9
f	acoustic frequency, hertz	p. 16
f_r	poroviscous relaxation frequency, hertz	p. 5

[a] An examination of the tables and figures that come from other authors reveals a large variation in symbols, units, and abbreviations for the same quantities. Individually, the authors are self-consistent. In general, we have not included all the possibilities.

f_{min}	frequency of minimum attenuation rate, hertz	p. 83
f_{max}	frequency of maximum attenuation rate, hertz	p. 83
F	complex resistance term of oscillatory motion of pore fluid	p. 29
G	shear modulus (rigidity), Pa	p. 14
g	sound speed gradient in the water, s^{-1}	p. 83
H	water depth, m	p. 82
H_w	water depth, m	p. 76
k_p	Hamilton's compressional wave attenuation constant, dB/m/kHz or dB/km/Hz	p.16
k_s	Hamilton's shear wave attenuation constant (same units as for k_p)	p. 21
k	Darcy coefficient of permeability, cm/s; also specific permeability (Stoll) (cm^2)	p. 30; 36
K_b	bulk modulus of frame, Pa	p. 36
K_f	bulk modulus of fluid, Pa	p. 36
K_r	bulk modulus of grains, Pa	p. 36
K_{SR}	real part of complex bulk modulus of the skeletal frame	p. 39
M_z	mean grain diameter, ϕ-units	p. 9
N_f	poroviscous frequency number	p. 29
n	power of frequency of nonlinear attenuation in sediments	p. 16
n	Poisson's ratio of skeletal frame	p. 39
p	percentage porosity	p. 8
Q	quality factor	p. 56
Q_p	quality factor of compressional vibration	p. 20
Q_s	quality factor of shear vibration	p. 20
R	receiver	p. 79

RD	receiver depth	p. 78
S	source	p. 79
SD	source depth	p. 78
SD	standard deviation	p. 8
SE	standard error of the mean	p. 9
U	group velocity	p. 42
$U_{\min}$	Airy phase of first mode	p. 42
V	wave velocity (general)	p. 21
V_b	velocity of compressional wave in bottom, m/s	p. 22
v_E	rod velocity of frame, m/s	p. 39
V_p	velocity of compressional waves in bottom	p. 10
v_p	velocity of compressional waves in bottom	p. 54
$V_p(1)$	velocity of compressional waves, 1 meter in depth in bottom	p.13
V_s	velocity of shear waves in bottom	p. 14
v_s	velocity of shear waves in bottom	p. 54
v_s	shear velocity of frame, m/s	p. 39
$V_s(1)$	shear wave velocity at 1 meter depth in bottom, m/s	p. 14
V_w	sound speed, m/s	p. 22
V_1, V_2	compressional wave velocities of first and second kind in sediment, m/s	p. 29
V_3	shear wave velocity in sediment, m/s	p. 29
VLF	very low frequency, hertz	p. 50
Z	depth in bottom, cm	p. 25

α	amplitude decay rate, Np/m	p. 56
α	attenuation, dB/km	p. 55
α_p	amplitude decay rate for compressional waves, Np/m	p. 20
α_p	attenuation of compressional waves, dB/m	p. 62
α_s	amplitude decay rate for shear waves, Np/m	p. 20
α_s	attenuation of shear waves, dB/m	p. 62
β	fractional porosity	p. 5
γ	specific gravity: γ_r grains, γ_f fluid (water)	p. 30, 65
δ	logarithmic decrement of frame vibration	p. 56
δ_E	logarithmic decrement for longitudinal vibrations	p. 39
δ_p	logarithmic decrement for compressional waves	p. 20
δ_s	logarithmic decrement for shear vibrations	p. 39
δ_s	logarithmic decrement for shear waves	p. 20
ε	attenuation, dB/km	p. 48
η	kinematic viscosity, m^2/s	p. 5
η'	absolute viscosity, dyn·s/cm^2	p. 30
θ_i	angle of incidence, degrees	p. 65
λ	wavelength, m	p. 22
$\Lambda_{m,n}$	mode (m,n) interaction wavelength	p. 43
μ	shear modulus of frame, Pa	p. 36

μ	microns (micrometers)	p. 19
ρ_b	bulk density of saturated bottom material, g/cm^3	p. 22
ρ_f	density of fluid, g/cm^3	p. 48
ρ_r	density of grains, g/cm^3	p. 9
ρ_s	saturated bulk density, g/cm^3	p. 9
ρ_w	density of pore water, g/cm^3	p. 9
σ_ϕ	sorting parameter in ϕ units	p. 31
ϕ	logarithmic unit of mean grain size	p. 9

I. INTRODUCTION

1. General

The objective of this study is to develop a procedure for experimentally isolating and quantifying the effects of the mechanisms controlling propagation of low frequency (20 to 500 Hz) signals in shallow water (20 to 200 m).

One of the main differences between shallow and deep ocean bottoms is the variety and thicknesses of sedimentary layers in shallow water.[1] The sedimentary cover serves either as an acoustic shield or as a coupler between the seawater and the hard rigid basement. The acoustic properties of the rigid basement underlying the sediments are thought to be well understood.

The Biot theory of the acoustic properties of sediments shows that there are important mechanisms that can control the sedimentary acoustics. Chief in importance is the flow permeability of seawater in saturated sediments. Next in importance are the sediment rigidity, or shear modulus, and skeletal frame loss. In this report, we shall investigate the importance of those mechanisms in the frequency range of interest.

2. Basement Structure in Shallow Water

To develop our point of view, we begin by briefly examining the "big picture." Figure I-1 shows an idealized diagram of the structure of the earth's crust in continental

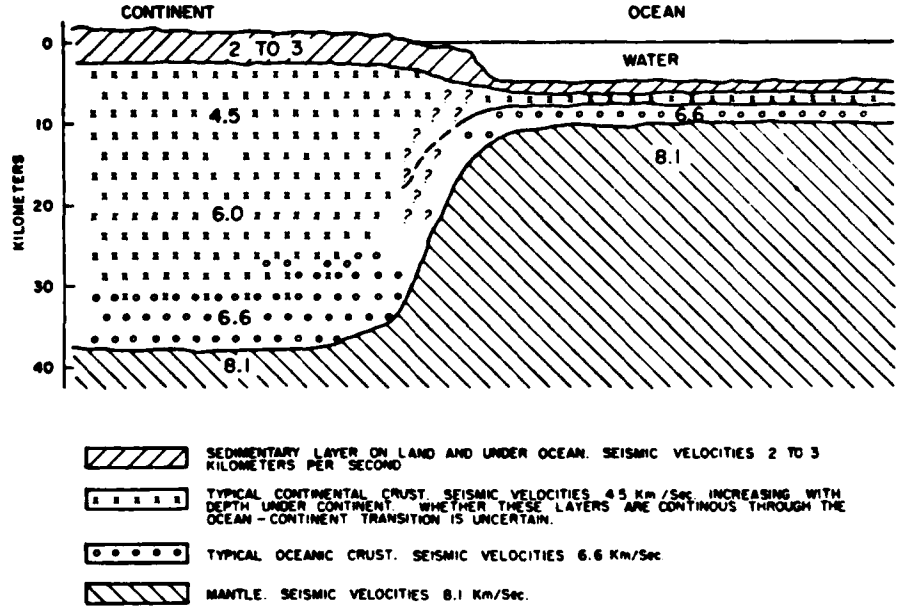

Fig. I-1. Idealized structure of the earth's crust. (Ref. 2)

and oceanic regions.[2] The various layers are labeled with the speed of propagation of compressional waves. For our purposes we shall mention only the upper two layers because these form the basement that underlies the sediments that are considered in this study. At a typical experimental site the first basement layer might be limestone that has a compressional wave velocity of 2.25 km/s and a shear wave velocity of 1 km/s. The second basement layer might be basalt with a compressional wave velocity of 5.25 km/s and a shear wave velocity of 2.5 km/s.

3. Formation of Shallow Water Sediments

In general, marine sediments are a heterogeneous collection of all the materials that are either carried into the sea or produced in it heavy enough to sink to the bottom, and inert enough not to dissolve or decompose in solution.[3]

A large proportion of the shallow water sediments originates on land. Direct erosion of the shoreline by wave action is one source. Rivers also drain and deposit their load of silt in the sea. Glacial movement is another source. Still other sources are airborne dust from arid regions and from volcanic explosions. The sea itself produces some of its bottom sediments by biological processes (e.g., shell and coral) and the precipitation of inorganic chemical substances from seawater.

The sea is continually moving and reworking the loads of sediment brought into it. Waves and currents carry the smaller particles along, grinding them against each other and against larger stationary objects on the bottom. Over long periods of time, boulders are transformed into mud, and chemical activity will further dissolve and decompose sedimentary materials. Some substances resist chemical and physical dissolution more than others. The hardness and inertness of quartz in the form of sand is responsible for its abundance on the continental shelf.

Since coarse particles from river outflow settle more quickly than fine particles, sediments tend to be coarse near shore, grading to mud or clay. The buoyancy of the water reduces friction between fine particles so that mud slides are fairly common whenever silt settles on a sloping bottom.

In the tropics, coral reef formation is often the dominant feature of submarine topography in shallow water. On the other hand, rough and rocky bottoms are found in the neighborhood of islands produced by submarine volcanic eruptions.

4. Bottom Acoustic Interaction in Shallow Water

For a given frequency and sound-speed profile, acoustic interaction with the bottom increases with decreasing water depth. Eventually, however, as the depth decreases, a cutoff frequency is reached below which the water column ceases to act as a waveguide. The cutoff frequency is inversely proportional to water depth, and in 100 m of water it is approximately 10 Hz. Below the cutoff frequency waterborne propagation is extremely poor, and interface and seismic waves can become important propagation paths.

Alternatively, as the wavelength increases, bottom interaction also increases so that some form of shallow water model must be used for the interpretation of acoustic propagation. For wavelengths of the order of the water thickness, it has been customary to characterize the water layer by an average value of sound speed. Pekeris[4] achieved success in compressional wave dispersion analysis using a two fluid layer model with constant speeds in the water and bottom. The next step[5,6] was to model the bottom as a lossy material with a constant compressional velocity and attenuation rate. After that, rigidity[6] was added to the bottom sediment properties to allow for shear wave conversion and attenuation. Eventually gradients for all parameters were included. Stoll and Bryan[7] pointed out the important properties of sediment acoustics arising from Biot theory.[8-10] According to this theory, sediments and porous rocks can be viewed as multiphase media: a solid, but imperfect elastic frame along with fluid pore water and gases. The

effects of fluid viscosity and soil anelasticity have been incorporated into existing propagation models as the complex velocities of the compressional and shear waves, but Yamamoto[11] obtained the exact analytical solution for the normal modes of the acoustic waves propagating in a homogeneous ocean overlying a homogeneous half-space of permeable material. The differences from viscoelastic theory at small grazing angles are important in determining the acoustic field in the water. The occurrence of a relaxation frequency, especially for sands at low frequencies, causes an attenuation rate falloff greater than the first power of frequency. There is also dispersion in the vicinity of the relaxation frequency.

5. Biot Factors

Important sediment parameters for understanding the consequences of the Biot theory are permeability, shear modulus, or rigidity, and skeletal frame loss. They are usually measured statically in the laboratory. They are difficult to measure experimentally *in situ*. Permeability is most important, being equal in importance to the choice of acoustic frequency. It enters into the determination of the relaxation frequency[11]

$$f_r = \frac{\beta\eta}{3\pi B},$$

where B is the specific permeability (m^2), β is the fractional porosity, and η is the kinematic viscosity (m^2/s). Note that there is an inverse relationship between porosity

and permeability in the expression for relaxation frequency. Thus the relaxation frequency increases with increasing porosity but decreases with increasing permeability. However, in natural sediments it is found that higher porosities correspond to lower permeabilities. Therefore, the relaxation frequency and the width of the relaxation peak provide a simple means of classifying sediments. While there is negative correlation between porosity and both mean grain size and permeability, the range of permeabilities is about five decades, going from 5×10^{-11} m^2 for coarse sand to 2×10^{-16} m^2 for silty clay. If we include limestone with a permeability of 5×10^{-10} m^2, the permeability range is extended to almost six decades. Porosity values only range from 30 to 90%. Thus one *may appreciate the importance* of measuring permeability *in situ*.

The shear modulus also requires better *in situ* determination. However, the excitation and measurement of water-seabed interface waves helps in this respect.[12] Yamamoto and Torii[13] have also shown how to get the shear modulus profile in the sediment using bottom motion induced by surface gravity waves.

In this paper, we shall discuss the importance of these Biot factors in relation to geoacoustic layer models, plane wave reflection coefficients, and propagation loss and optimum frequency.

II. GEOACOUSTIC PARAMETERS

1. Sediment Surface Properties

Sediment surface properties for sands, silts, and clays, based on the Shepard[14] nomenclature diagram, are shown in Tables II-1 and II-2, which were presented by Hamilton at a shallow water workshop in 1983.[15] They are not much different from a previous summary by Hamilton.[16] The tables contain averaged results of measurements and computations of acoustic and related properties for continental terrace (shelf and slope) sediments made by the Naval Ocean Systems Center up to November 1982. These data are for the upper 30 cm of the seafloor. *In situ* measurements were made with probes and diver grab samples, in addition to those from cores. Sound velocity values have been

Table II-1. Continental terrace (shelf and slope) environment; average sediment size analyses and bulk grain densities. (Ref. 15)

Sediment Type	No. Samples	Mean Grain Size mm	Mean Grain Size ϕ	Sand, %	Silt, %	Clay, %	Bulk Grain Density, g/cm^3
Sand							
Coarse	2	0.5285	0.92	100.0	0.0	0.0	2.710
Fine	28	0.1638	2.61	92.2	4.1	3.7	2.709
Very Fine	16	0.0988	3.34	81.0	12.5	6.5	2.680
Silty sand	40	0.0529	4.24	57.0	30.9	12.1	2.677
Sandy silt	47	0.0340	4.88	30.3	57.8	11.9	2.664
Silt	19	0.0237	5.40	7.8	80.1	12.1	2.661
Sand-silt-clay	29	0.0177	5.82	31.7	42.9	25.4	2.689
Clayey silt	105	0.0071	7.13	7.4	58.3	34.3	2.656
Silty clay	54	0.0022	8.80	3.9	34.8	61.3	2.715
					average	=	2.678

Table II-2. Continental terrace (shelf and slope) environment; sediment densities, porosities, compressional sound velocities, and velocity ratios.[a] (Ref. 15)

Sediment Type	Density, g/cm^3 Avg.	SE	Porosity, % Avg.	SE	Velocity, m/s Avg.	SE	Velocity Ratio Avg.	SE	Acoustic Impedance Ratio[b]
Sand									
Coarse	2.034	--	38.6	--	1836	--	1.201	--	2.443
Fine	1.962	0.017	44.5	1.0	1759	9	1.152	0.006	2.260
Very fine	1.878	0.017	48.5	1.0	1709	14	1.120	0.009	2.103
Silty sand	1.783	0.014	54.2	0.8	1658	7	1.086	0.005	1.936
Sandy silt	1.769	0.018	54.7	1.1	1644	7	1.076	0.004	1.903
Silt	1.740	0.027	56.2	1.6	1615	6	1.057	0.004	1.839
Sand-silt-clay	1.575	0.021	66.3	1.4	1582	7	1.036	0.005	1.632
Clayey silt	1.489	0.014	71.6	0.7	1546	3	1.012	0.002	1.507
Silty clay	1.480	0.010	73.0	0.5	1517	2	0.990	0.001	1.465

[a] Laboratory values, 23°C, 1 atm; density, saturated bulk density; porosity, salt free; velocity ratio is velocity in sediment/velocity in seawater at 23°C 1 atm, and salinity of sediment pore water; SE, standard error of the mean; standard deviation, SD, can be computed with SD = (SE)(no. samples)$^{1/2}$. Median values [rather than mean (avg.) values] are recommended for predicting values for clayey silt. These are: density, 1.484 g/cm^3; porosity, 72.5%; velocity, 1534 m/s; velocity ratio, 1.006 (see text for discussion).

[b] Added by authors.

corrected to 23°C and 1 atm pressure, using tables for the speed of sound in seawater. In reality these classes grade continuously into one another and are meant to be only representative.

2. Porosity vs Mean Grain Size

The porosity, p(%), of a saturated sediment is defined as that percentage of the total sediment volume that is occupied by water. The size of the sediment mineral grains is

usually expressed by the parameter M_z defined by

$$M_z = -\log_2 d \ ,$$

where d is the mean grain size (diameter) in millimeters and where the units of M_z are denoted ϕ. The following empirical relationship between p and M_z has been found to be useful.

$$p\,(\%) = 22.01 + 9.24\,M_z - 0.365\,M_z^2 \qquad SE = 6.5\% \ .$$

It is noted in passing that nonuniformity of grain size (sorting), grain shape, the packing of the grains, and the grain mineralogy increase the standard error (SE).

3. Density

The saturated bulk density of a gas-free sediment is given by

$$\rho_s = \beta\rho_w + (1-\beta)\rho_r \ ,$$

where β = fractional porosity, ρ_w = density of pore water, and ρ_r = bulk density of mineral grains. The saturated bulk density (g/cm^3) can be related to porosity p and mean grain size M_z (in ϕ-units) by the following empirical relations.

(1) $p\,(\%) = 157.6 - 57.8\,\rho_s$ SE = 2.1%

(2) $\rho_s = 2.374 - 0.175\,M_z + 0.008\,M_z^2$ SE = 0.11g/cm^3

4. Compressional Wave Velocity

Three regression equations are given for compressional wave velocity as functions of (a) porosity, (b) saturated bulk density, and (c) mean grain size.

(a) Compressional wave velocity vs porosity, p (%)

$$V_p \text{ (m/s)} = 2502 - 23.45p + 0.14p^2 \quad \text{SE} = 31 \text{ m/s}$$

(b) Compressional wave velocity vs saturated bulk density, ρ_s (g/cm^3)

$$V_p \text{ (m/s)} = 2330.4 - 1257.0\,\rho_s + 487.7\,\rho_s^2 \quad \text{SE} = 33 \text{ m/s}$$

(c) Compressional wave velocity vs mean grain size, M_z (ϕ - units)

$$V_p \text{ (m/s)} = 1952.5 - 86.26M_z + 4.14M_z^2 \quad \text{SE} = 29 \text{ m/s}\,.$$

Figures II-1 and II-2 (Hamilton[17]) present plots of compressional wave velocity vs

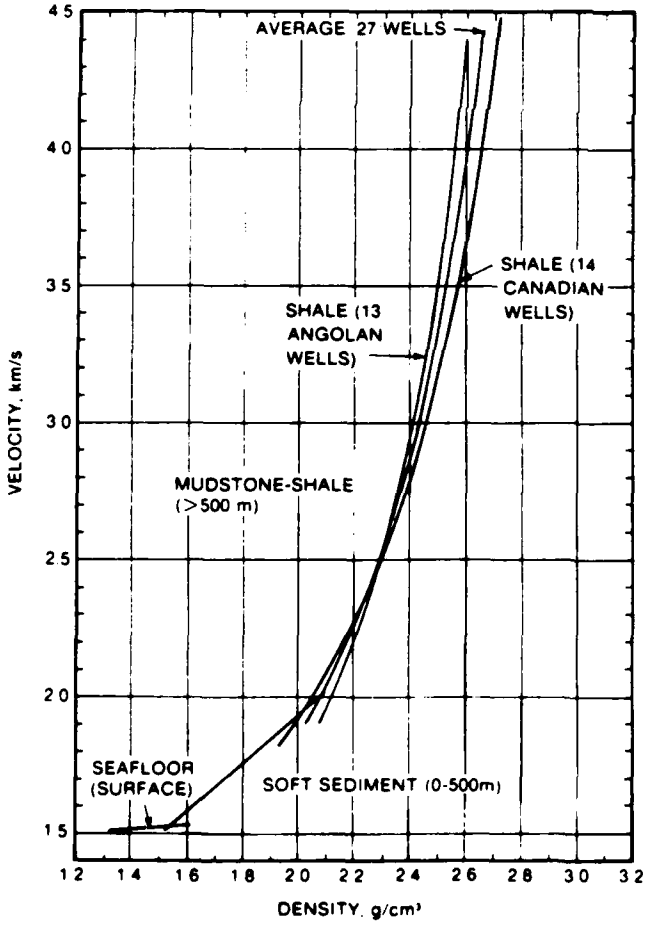

Fig. II-1.
Compressional wave (sound) velocity versus saturated bulk density in marine sediments (silt-clays, turbidities) and sedimentary rocks (mudstone, shale) from terrigenous sources. See Hamilton[17] for references, regression equations, and discussions. (Ref. 17)

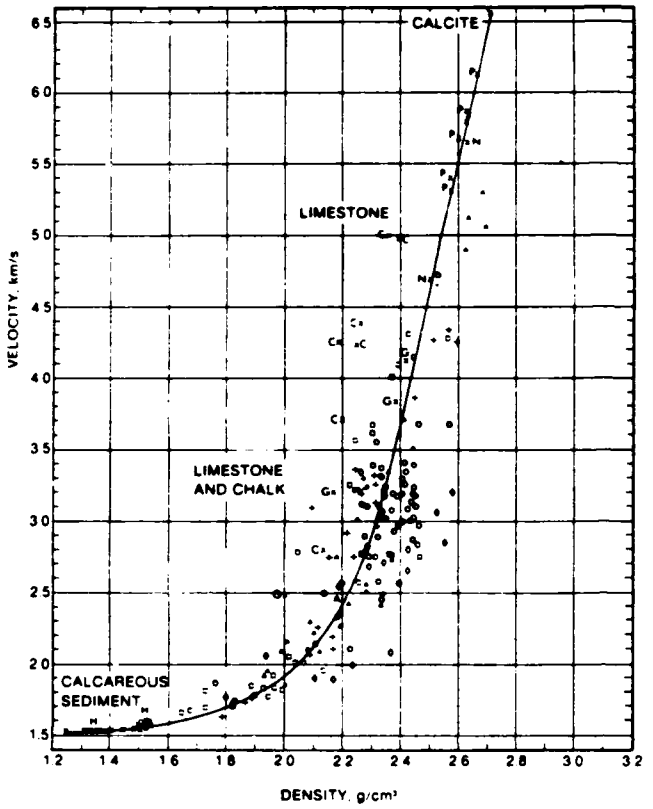

Fig. II-2.
Compressional wave (sound) velocity versus saturated bulk density in marine calcareous sediments and rocks. See Hamilton[17] for references, regression equations, and discussions. (Ref. 17)

saturated bulk density, for silty clays and turbidities, and for calcareous sediments, respectively.

5. Compressional Wave Velocity Gradients in Depth

The gradient in depth of sediment compressional wave velocity is important because it affects the amount of acoustic energy returned to the water. These gradients are normally positive and cause acoustic energy to be refracted upward through sediment layers and returned to the water. As a result it is possible to compute layer thicknesses and densities, and to infer information regarding consolidation and lithification characteristics of sediment mass.

Values of velocity gradients at the surface in silty clays range from 0.7 s^{-1} to 1.99 s^{-1}. Supposing a value of 1.28 s^{-1} at the seabed, the positive gradient will typically decrease to about 0.58 s^{-1} at a depth of 1 km.

Factors causing velocity gradients in silty clay sediments to a depth of about 500 m are:

(a) pressure-induced porosity reductions which result in an increase in the saturated density and effects on sediment mineral frame (66% of gradient),

(b) temperature increases due to heat flow (17% of gradient),

(c) increases in mineral-frame rigidity caused by lithification (15% of gradient),

(d) pore-water pressure increases (2% of gradient).

These percentages add up to 100% but are only estimates and will vary with sediment type, depth, and age. Age enters because time is an element in rates of sedimentation, consolidation, and the duration of time required to allow maximum cohesion and cementation between mineral grains (lithification).

Smaller velocity gradients will be present in silty clay sediments of the continental terrace (shallow water), especially on or near river deltas, where sediments accumulate rapidly and have not had time to consolidate fully. A typical velocity gradient for silty clays on the U.S. coast is about 0.90 s^{-1}.

In sand, the sound velocity increases very fast in the first few meters. The gradient then decreases sharply after the initial rapid increase. In sands, there is little significant reduction of porosity caused by pressure in the upper tens of meters of the sediment. The main effects on sound velocity are due to the rigidity of the sand mineral structure caused by intergranular pressure. Effects of hydrostatic pressure in the pore water and temperature gradients are not significant at shallow depths.

Depth dependence of compressional wave velocity in sands follows the law $V_p = V_p(1)D^{0.015}$ (Ref. 18), where D is the depth in meters and $V_p(1)$ is the reference velocity in m/s at a depth of 1 m. For a sand reference velocity of $V_p(1)$ = 1806 m/s we find:

Depth, m	Compressional Wave Velocity, m/s	Velocity Gradient, s^{-1}
1	1806	27.1
2	1825	13.7
10	1869	2.8
20	1889	1.4

6. Shear Wave Velocities and Gradients in Depth

The effects of sediment rigidity can also be important for long-range sound propagation. In thin sediment layers, over a consolidated rigid bottom, conversion of compressional waves to shear waves and interface waves at the sediment-basement boundary can

be an important energy loss mechanism. Energy losses from such conversions are usually less at other reflection boundaries such as the seafloor and at internal reflectors.

Empirical relations for shear wave velocities (m/s) versus depth (meters) in sediments for two important sediment types, sands and silty clays, have been reviewed by Hamilton.[18]

Sands: $V_s = 128D^{0.28}$ m/s (D, meters)

Silty Clays:
$$\begin{cases} V_s = 116 + 4.65D & (0\text{–}36\ \text{m}) \\ V_s = 237 + 1.28D & (36\text{–}120\ \text{m}) \\ V_s = 322 + 0.58D & (120\text{–}650\ \text{m}) \end{cases}$$

Ohta and Goto[19] give the following expression for shear velocity (m/s) versus depth, D, (m) for sediments.

$$V_s = V_s(1) D^{0.312}.$$

This expression is used in calculating Table II-3.

Table II-3. Calculation of shear properties of sediments.

Bottom Type	$V_s(1)$ m/s	Velocity Gradient at 1 m, s^{-1}	Depth, m, to V_s = 600 m/s	Shear[a] Modulus at 1 m G, N/m^2
Gravel	178.1	55.6	49.0	8.41×10^7
Sand and gravel	129.6	40.4	136.0	4.45×10^7
Coarse sand	112.3	35.0	215.0	2.56×10^7
Medium sand	101.3	31.6	300.0	2.01×10^7
Fine sand	99.51	31.0	317.0	1.86×10^7
Silts and clays	78.98	24.6	664.0	0.929×10^7

[a] $G = \rho V_s^2$

7. Attenuation of Compressional Waves

A. Intrinsic Attenuation

When sound energy passes through a homogeneous, isotropic, porous saturated sediment, energy is lost because of friction between mineral grains, and by viscous losses owing to the relative movement of pore water through the mineral frame. This is called intrinsic attenuation.

B. Effective Attenuation

At low frequencies and deep penetration into the sediments, effective attenuation is due to a number of causes.

(1) Intrinsic absorption or attenuation.

(2) Interface losses.

(a) Conversion of compressional waves to shear waves and interface waves with rapid attenuation.

(b) Attenuation owing to intrabed multiple reflections (frequency dependent).

(3) Reflector surface roughness and curvature.

(4) Scattering by inhomogeneities.

In sediments the compressional wave attenuation in decibels per meter is often given by $a_p = k_p f^n$, where f is frequency in kilohertz and k_p is a constant for a given sediment type; when $n = 1$, k_p is in decibels per meter per kilohertz. k_p has been determined as a function of mean grain size or porosity. For silts and clays, a dependence on the first power of frequency (f^1) is found for a_p (Refs. 7, 16, and 20-22). For sands, this behavior is found from 1 to 100 kHz. But Stoll and Bryan[7] and Stoll[21,22] find, following Biot, that a_p varies as f^2 at very low frequencies and as $f^{1/2}$ at very high frequencies. There is an inflection point at the relaxation frequency between 1 and 20 kHz for sands. The actual frequency dependence depends on the competition between the first power law of skeletal frame loss and the frequency behavior of the loss due to the relaxation process.

Hovem[23] and Hovem and Ingram[24] find that energy losses due to the relative motion of the pore water and the sediment mineral frame lead to f^2 attenuation at low frequencies and may be of potential importance only in sound propagation in sands with uniform grains and high permeability.

Hamilton has found that in surface sands, assuming that $n = 1$, k_p values range from 0.25 to 0.60, with the best data giving about 0.5. Figure II-3 is a plot of Hamilton's attenuation factor, k_p, for compressional waves in decibels per meter per kilohertz versus porosity in percent. For convenience Hamilton has fitted the data against porosity in the four regions shown.[20] The equations of the lines are presented in the inset.

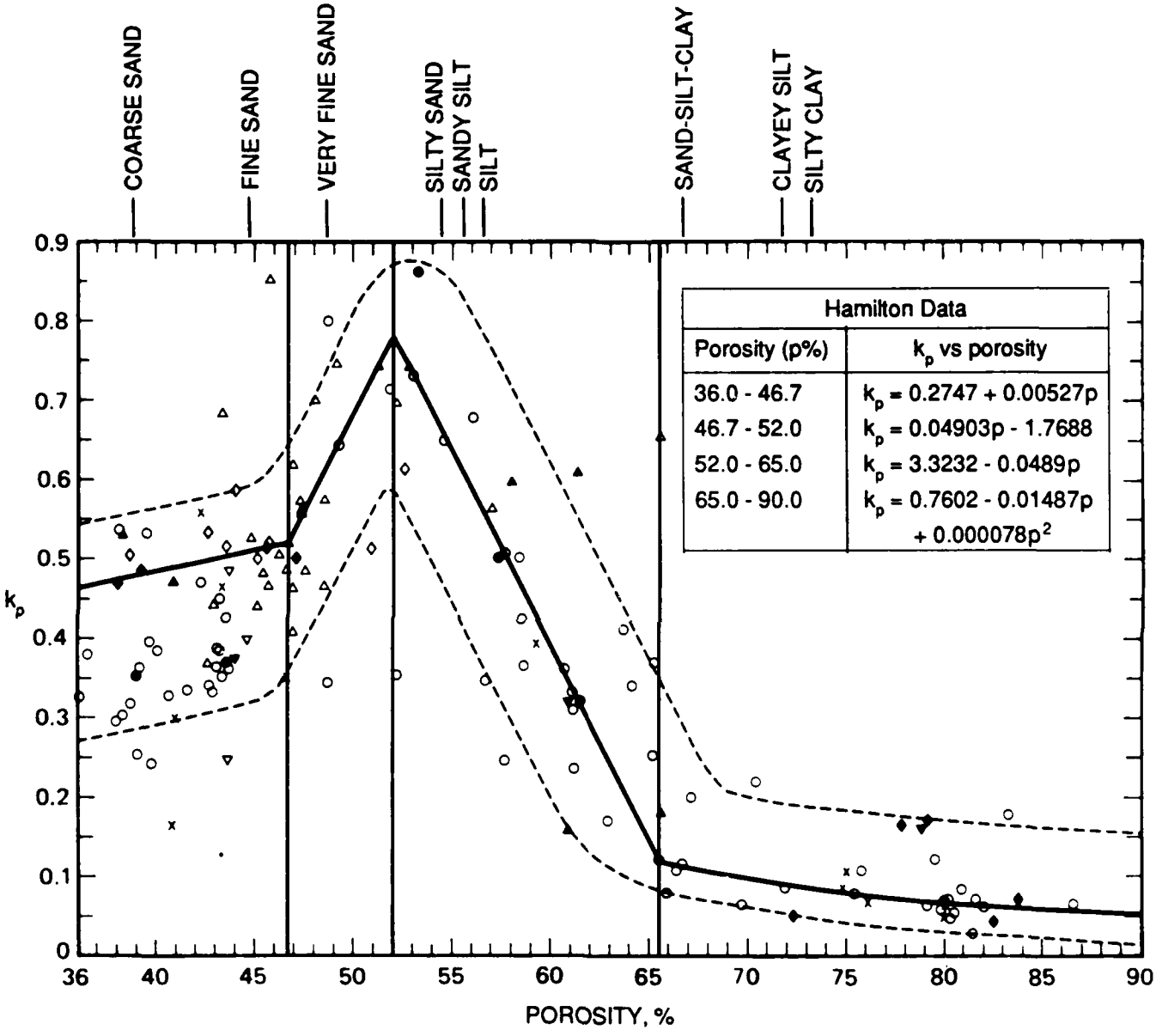

Fig. II-3. Attenuation of compressional waves (expressed as k_p, where $a_p = k_p f$ in dB/m, where frequency, f, is in kHz) versus porosity in natural, saturated surface sediments. Solid symbols are averages and open symbols are the averaged data from measurements off San Diego; solid lines are regressions on the best data. (Ref. 20)

Figure II-4 is a plot of k_p versus mean grain size. Note that the sharp rise at about $\phi = 6$ emphasizes the difference between the clays (soft sediments) and silts and sands. See also later Figure III-4 where the separation between a first power law with frequency is shown to occur at this mean grain size.

C. Attenuation of Compressional Waves with Depth in Seafloor

Available data on the depth dependence in the seafloor of compressional wave attenuation is shown in Figure II-5.[16,18] For sands, Hamilton suggests $k_p = 0.45D^{-1/6}$, where D is depth in meters in the seafloor and k_p is in decibels per meter per kilohertz (Ref. 16). There is an apparent tendency for k_p to increase with depth down to a few hundred meters for silty clays. Neprochnov[25] classified layer types for thick sediment and rock layers for the frequency range 20 to 200 Hz: (1) first type layers: unlithified sediments (200 to 400 m); (2) second type layers: sedimentary rock (800 to 1400 m); (3) third type layers: sedimentary rock and basalts (1500 to 2200 m). Mitchell and Focke have treated attenuation of compressional waves with depth in the seafloor in a definitive fashion.[26]

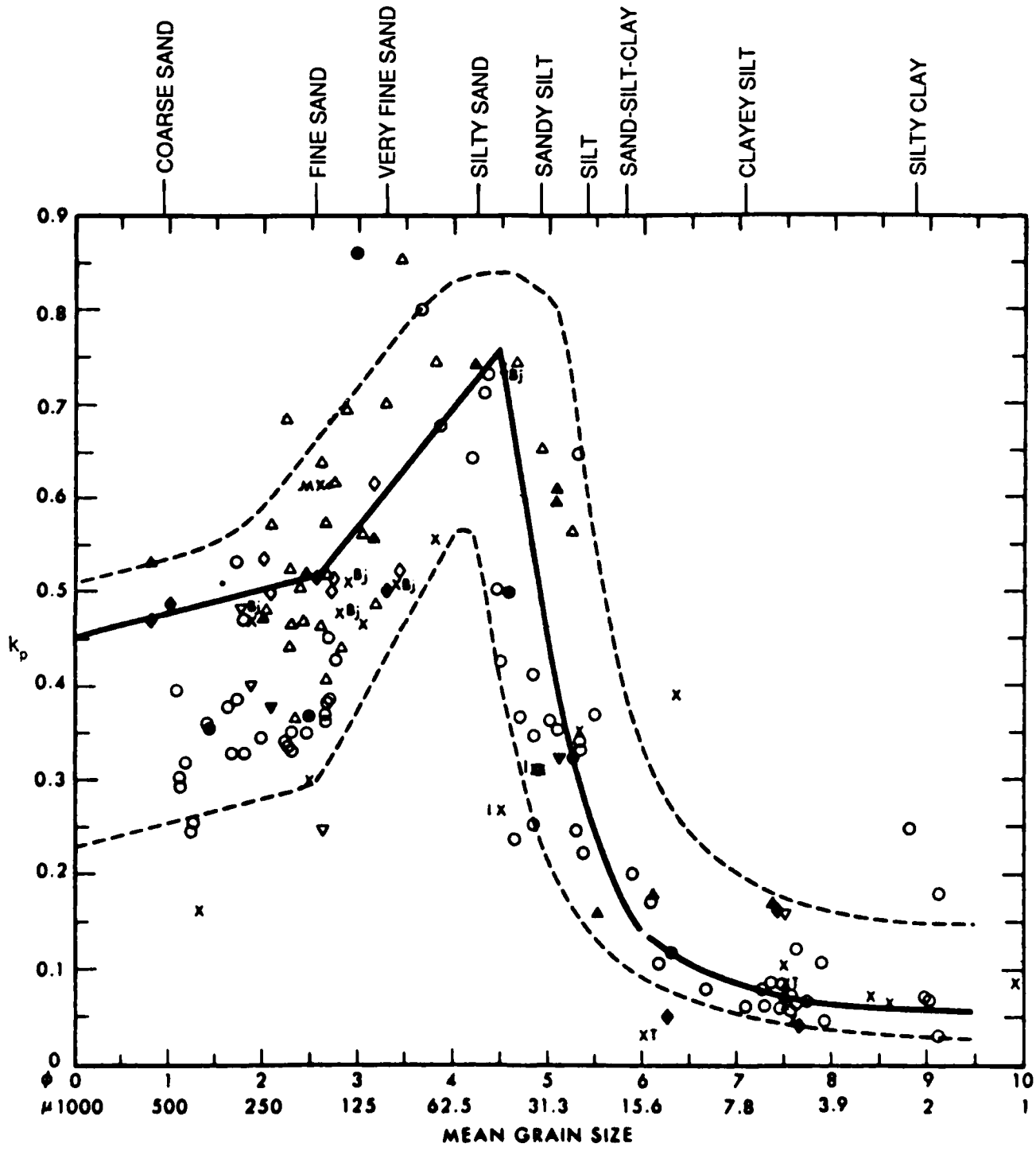

Fig. II-4. Surface-sediment mean grain size versus attenuation of compressional waves expressed as k_p. See Hamilton[20] for additional information and regression equations.

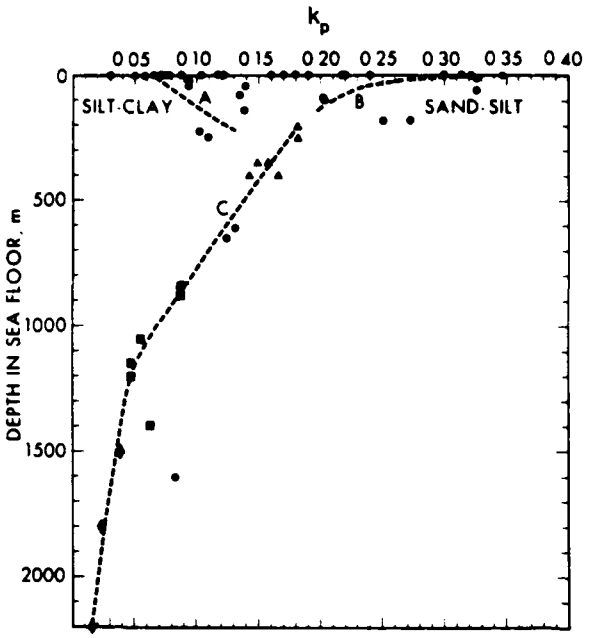

Fig. II-5.
Attenuation of compressional waves (expressed as k_p in a_p (dB/m) = $k_p f$; where frequency, f, is in kHz) versus depth in the seafloor, or in sedimentary strata; see Hamilton[18] for discussions where symbols A, B, and C are explained. (Ref. 18)

8. Attenuation of Shear Waves

Logarithmic decrement, δ, is often used as a measure of acoustic energy loss, just as it is in vibration analysis and in soil mechanics and foundation engineering.

$$\delta_{p,s} = \frac{\pi}{Q_{p,s}} = \frac{\alpha_{p,s} V_{p,s}}{f},$$

where

$\delta_{p,s}$ ≡ logarithmic decrement (natural log of the ratio of two successive amplitudes in an exponentially decaying sinusoidal wave); notation p,s stands for either compressional (p) or shear (s) waves

$Q_{p,s}$ ≡ quality factor of vibration (inversely proportional to the fractional energy loss per cycle)

$\alpha_{p,s}$ ≡ amplitude attenuation coefficient, Np/m

$V_{p,s}$ = wave velocity (compressional or shear), m/s

f = frequency, Hz

$a_{p,s}$ = $8.686\alpha_{p,s}$ dB/m (intensity attenuation coefficient) = $8.686\ \delta_{p,s}\ (f/2V_{p,s})$

$k_{p,s}$ = $a_{p,s}/f$

Hamilton recommends k_s be assumed constant for low strain ($\sim 10^{-5}$) shear waves. He recommends for near surface *natural sands* that $\delta_s \approx 0.30 \pm 0.15$. Similarly for silty-clay sediments, he recommends $\delta_s \approx 0.2 \pm 0.1$.

Assuming that attenuation of low-strain shear waves is proportional to the first power of frequency (which has not been proven in sands) some of the shear wave energy-loss data from the literature can be placed in the form: $a_s = k_s f$, where the intensity attenuation of shear waves, a_s, is in decibels per meter; frequency, f, is in kilohertz; and k_s is a constant in decibels per meter per kilohertz.

For geoacoustic modeling of viscoelastic bottom materials, Table II-4 gives a summary of some parameters for both compressional and shear waves. These values were obtained and verified semiempirically with fits to propagation data and theoretical models.[27,28] Note the convention of giving attenuations, a_λ, in decibels per wavelength. This is equivalent to assuming that attenuation is proportional to frequency.

Shear-wave attenuation for silt-clays varies with depth in the seafloor similarly to compressional wave attenuation below the value that occurs at roughly 280 m (see Figure II-5). The depth dependence of shear wave attenuation in silt-clays and sands is $k_s \sim D^{-1/6}$, the same as for compressional waves.

Table II-4. Geoacoustic parameters for different bottom types. (Refs. 27, 28)

Bottom Type	Porosity p (%)	Relative[a] bulk density ρ_b/ρ_w	Relative[b] speed V_b/V_w	Compressional wave speed V_b (m/s)[a]	Shear velocity V_s (m/s)	Compressional wave attenuation $a_{p\lambda}$ (dB/λ_p)	Shear wave attenuation $a_{s\lambda}$ (dB/λ_s)
Clay-silt	60	1.6	1.01	1515	100	0.5	1.0
Sand-silt-clay	55	1.7	1.02	1530	150	0.8	1.5
Silt	50	1.8	1.05	1600	200	1.0	2.0
Sand-silt	40	1.9	1.1	1650	400	0.8	1.5
Coarse sand	35	2.0	1.2	1800	600	0.7	1.5
Chalk-limestone	--	2.2	1.5	2250	1000	0.4	1.0
Limestone	--	2.4	2.0	3000	1500	0.3	0.5
Basalt	--	2.6	3.5	5250	2500	0.2	0.5

[a] subscript b is for bottom; w is for water
[b] V_w = 1500 m/s

9. Density Gradients

Acoustic reflection surveys are used to delineate sediment and rock layers of the seafloor. Wide-angle reflection and refraction measurements (as with expendable sonobuoys, or multichannel, long-streamer technology) also yield sound velocities in these layers. Frequently the underlying rock types can be identified from boreholes, extrapolation from onshore geology, or through geological reasoning. The velocity versus depth data can then be used to estimate density versus depth through velocity-density relations. Hamilton[17] presents two methods for obtaining values of density versus depth. In thicker sections where there are sound velocity data, the velocity-density relations for the appropriate sediment-rock type can be used with a core measurement. The other method is to take a value of density from surface core measurements and apply an appropriate gradient from generalized studies.

10. Probes for the Measurement of Seafloor Properties

Reliable measurements of seafloor sediment properties are required for geoacoustic modeling. Standard sampling and testing methods, particularly when applied in sands, often do not provide sufficiently reliable sediment property measurements for dependable, economical sediment performance prediction. *In situ* measurement capabilities at NORDA presently include sediment pore water pressure, shear strength, electrical conductivity, and compressional and shear wave velocities.[29,30] Current developments include:

(a) Diver-operated conductivity probe that measures directly sediment conductivity, temperature, and probe penetration below the seafloor. Such measurements yield sediment porosity and bulk density.

(b) A piezometer probe to measure excess pore pressures generated by probe insertion at a water depth of 5800 m. The excess pore pressures generated by insertion of the probe can be interpreted to classify the sediment type and to estimate sediment permeability, porosity, and undrained shear strength.

(c) Diver-operated compressional wave velocity probes (70 kHz) have been developed and shear wave velocity probes (2 kHz) are being developed (see Figure II-6).

ACTIVE END OF
COMPRESSIONAL WAVE PROBE

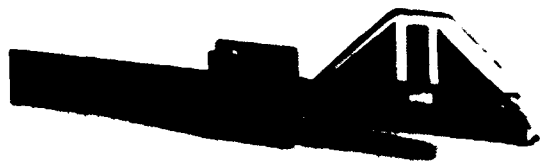

ACTIVE END OF
SHEAR WAVE PROBE

MEASURES DIRECTLY: COMPRESSIONAL WAVE VELOCITY
COMPRESSIONAL WAVE ATTENUATION
SHEAR WAVE VELOCITY

MEASURES INDIRECTLY: SEDIMENT: BULK MODULUS
SHEAR MODULUS
YOUNG'S MODULUS
POISSON'S RATIO

FEATURES: 1. FREQUENCY: COMPRESSIONAL~70 kHz, SHEAR~2 kHz
2. GOOD COUPLING IN SOFT SEDIMENTS
3. CAN BE EMBEDDED IN SANDS WITH MINIMAL DISTURBANCE

USES: GEOACOUSTIC MODEL INPUTS
EMPIRICAL DATA ON Vp/Vs RATIOS

Fig. II-6. Compressional and shear wave probes. (Ref. 29)

Compressional and shear wave velocity data (see Figure II-7), when combined with bulk density data obtained from the conductivity probe, permit a complete description of the sediment elastic properties for use in acoustic bottom interaction models. The sediment elastic properties are: bulk modulus, shear modulus, Young's modulus, and Poisson's ratio.

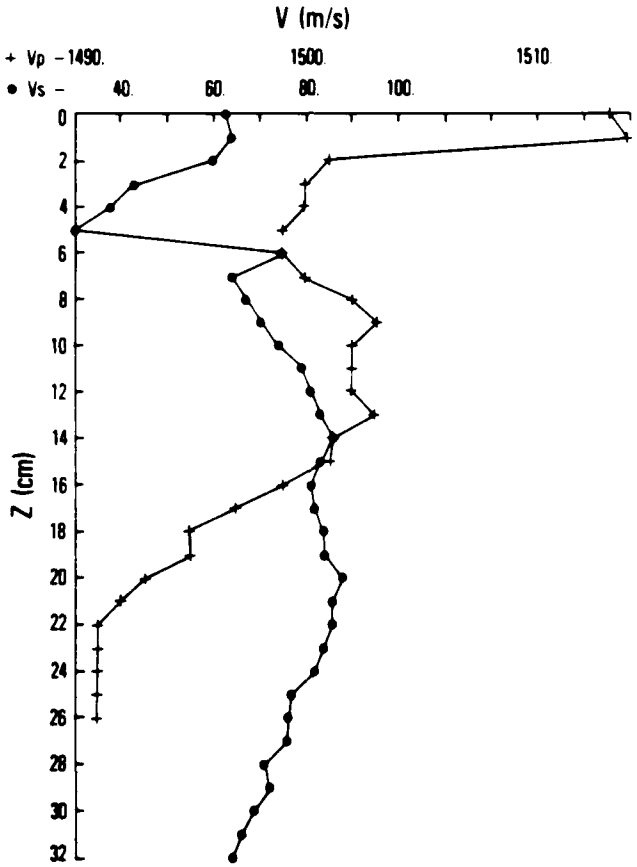

Fig. II-7. Compressional and shear wave velocities versus depth taken in a box core. Deep sea carbonate ooze. (Ref. 30)

III. BIOT THEORY

1. Introduction

Stoll and Bryan,[7] Stoll,[21] Yamamoto,[11] and McDaniel and Beebe[31] have shown that, at low acoustic frequencies when Biot theory is applied as opposed to the assumption of a fluid model or even a viscoelastic bottom model, numerical predictions for poro-viscous bottoms are different.

Biot's theory of the acoustic response of linear, porous materials containing a compressible pore fluid calls for two types of losses. There are losses due to the movement of the fluid relative to the skeletal frame, and losses due to the anelasticity of the frame. Viscous effects are treated using a frequency dependent factor for the flow resistance. In addition, complex bulk and shear moduli are used for the frame. Three types of propagating waves are found in the saturated sediment. There are two compressional waves and a shear wave. The second compressional wave travels very slowly, is highly attenuated, and usually exists at an interface.

There are several consequences of this theory that are different from those of the customary viscoelastic models. The theory, as interpreted by Yamamoto,[11] calls for a relaxation process that controls the compressional and shear attenuation rates and the magnitude of dispersion, and causes a nonlinear frequency dependence of the attenuation in sandy sediments at low frequencies. In fact, the relaxation frequency forms a natural

dividing line between "low" and "high" frequency.[24] Taking the relaxation process alone, as the frequency increases toward infinity, the frequency dependence approaches $f^{1/2}$ in behavior; as the frequency approaches 0, the frequency dependence behaves as f^2. In the broad neighborhood of the relaxation frequency, where the attenuation rate is a maximum, we expect a linear dependence on frequency. This linear frequency dependence is extended by the distribution of grain sizes that occurs in any natural sediment. Actually the linear dependence of attenuation on frequency normally observed is due to the skeletal frame loss which competes with the relaxation loss.

2. Relaxation Frequency

Yamamoto[11] finds that the two most critical bottom parameters for acoustic attenuation are the shear modulus (rigidity, G) and the relaxation frequency (f_r). The rigidity, G, is important when high speed (>550 m/s) shear waves are generated. When G is greater than 5×10^7 N/m^2, compressional wave energy is converted efficiently into shear waves with significant losses over and above those caused by the attenuation of fast compressional waves. The relaxation frequency (Hz) is given by

$$f_r = \frac{\beta\eta}{3\pi B},$$

where β is the fractional porosity, η is the kinematic viscosity (m^2/s), and B is the specific permeability (m^2). The maximum attenuation rate occurs for all three wave

types when $f = f_r$. Figure III-1[11] is a plot summarizing the relaxation behavior for a saturated sand. Note that the peak loss occurs within our stated frequency range of interest, 20 to 500 Hz.

The relaxation frequency f_r is controlled by the ratio β/B. Both the porosity, β, and the permeability, B, can be expressed as empirical functions of mean grain size. The kinematic viscosity of water, η, is a constant and equal to 1.0×10^{-6} m^2/s. McDaniel and Beebe[31] have developed an expression for permeability using mean grain size based on work by Krumbein and Monk.[32] There is also a Kozeny-Carman[33] constant relating permeability to grain size.

3. Permeability

Permeability is a measure of the relative ease with which a fluid will flow through soils. In general, voids in soils are connected to neighboring voids. Since the pores are interconnected, water can flow through the densest of natural soils. Permeability depends on the properties of both the permeant and the soil. Viscosity, density, and polarity are the important permeant properties. Particle size, void ratio, composition, fabric, and the degree of saturation are the major soil properties on land.

Soil permeability can be measured either in the laboratory or in the field. Since permeability depends on soil fabric, including microstructure and microstructure com-

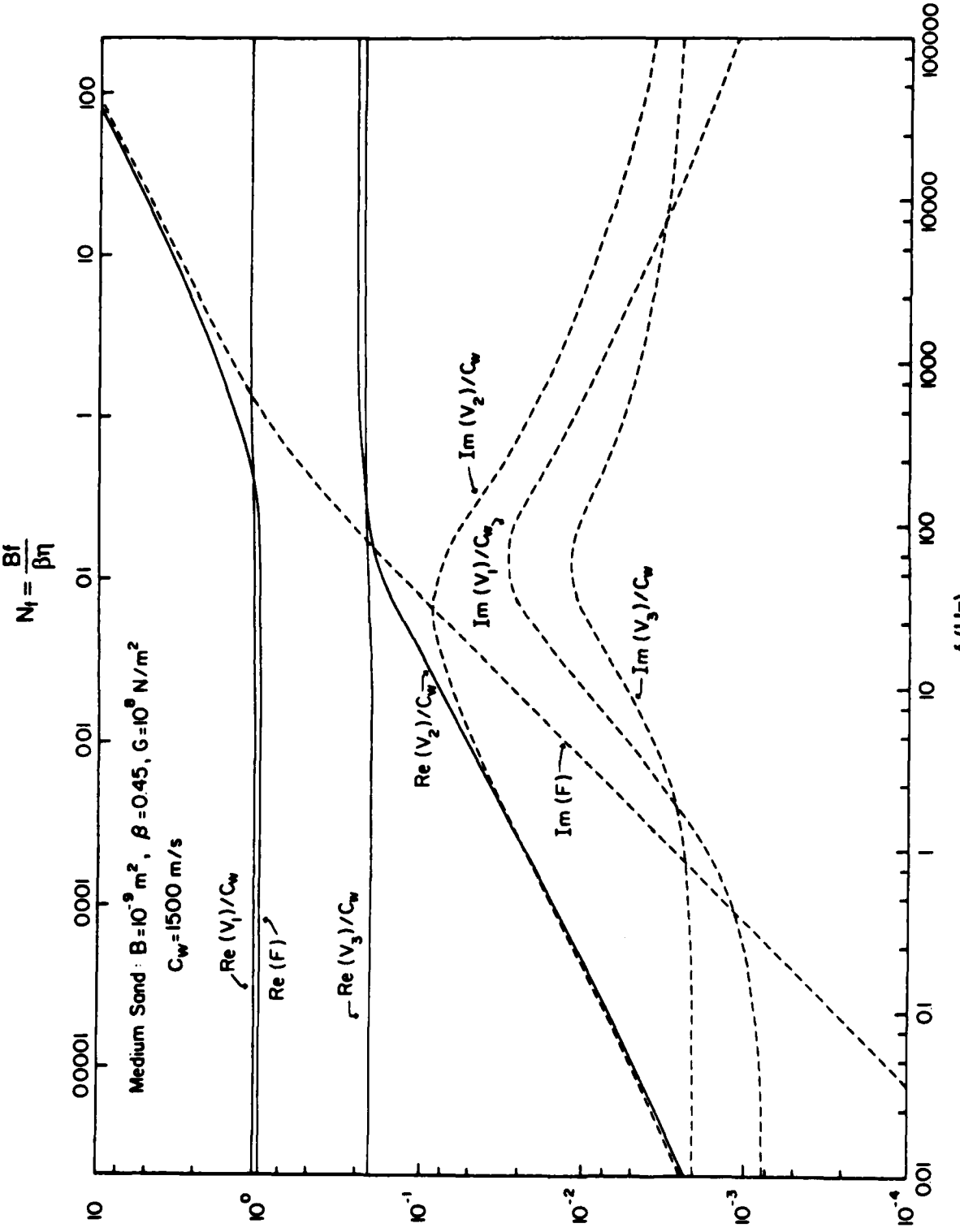

Fig. III-1. Effects of the poro-viscous frequency number, $N_f = Bf/\beta\eta$, on the velocity and attenuation of the three elastic waves in sediments. Re(V_1), Re(V_2), and Re(V_3) are the velocities of the fast compressional wave, the slow compressional wave, and the shear wave, respectively. Im(V_1), Im(V_2), and Im(V_3) are the corresponding attenuation constants. Re(F) and Im(F) are the viscous resistance term and the inertia resistance term of the oscillatory motion of pore fluid. C_w is the sound velocity in water. (Ref. 11)

ponents, and since it is difficult to get undisturbed soil samples, field determinations of permeability are often required to get a good measure of average permeability.

The range of permeability in sediments is quite large, extending from 1 cm/s for gravel, to below 10^{-8} cm/s for clay. While these units are velocity according to Darcy's original definition, it is customary in sediment acoustics to use the specific or absolute permeability which has the units of length squared. The specific or absolute permeability is defined as[34]

$$B = \frac{k\eta'}{\gamma},$$

where k is the Darcy coefficient of permeability (cm/s), η' is the absolute viscosity (dyne-s/cm^2) of the permeant, and γ is the specific gravity of the permeant. For water at 20°C, B is given by

$$B\,(\mathrm{cm}^2) = k\ (\mathrm{cm/s}) \times 1.02 \times 10^{-5}\ (\mathrm{cm \cdot s}).$$

From work on sands, Hazen proposed

$$k\ (\mathrm{cm/s}) = 100\ (\mathrm{cm \cdot s})^{-1}\, d_{10}^2\ (\mathrm{cm}^2),$$

where d_{10} (cm) is the diameter at which 10% of the soil is finer. To convert Hazen's expression to specific permeability,

$$B = 1.02 \times 10^{-3}\, d_{10}^2, \quad (\mathrm{cm}^2 \text{ or } \mathrm{m}^2, \text{ depending on the units of } \mathrm{d}_{10}).$$

Yamamoto[11] uses $B = 0.01\, d_{10}^2$. For fine sand $d_{10} = 0.1$ mm or 10^{-4} m yielding $B = 10^{-10}$ m^2, but this is too large by a factor of 10.

The McDaniel and Beebe expression for permeability includes a sorting term, σ_ϕ, in ϕ-units, to get from the mean grain size, in millimeters to d_{10}:

$$B\ (\mathrm{cm}^2) = 7.6\, d^2 \exp(-1.31\sigma_\phi) \times 10^{-6}\ ,$$

where d is the mean grain diameter in millimeters. The sorting, σ_ϕ, is given by

$$\sigma_\phi = \begin{cases} 0.773 M_z^{-0.272}, & 0.1\phi \le M_z \le 2.2\phi \\ 0.252 M_z^{1.112}, & 2.2\phi \le M_z \le 10\phi\ . \end{cases}$$

McDaniel and Beebe[31] have also developed two other expressions for sediment properties based on mean grain size: (1) saturated bulk density, ρ_s, and (2) porosity, p (%).

$$\rho_s = 2.149 - 0.0864 M_z\ , \qquad \mathrm{g/cm}^3$$

where M_z is the mean grain diameter in ϕ-units, and

$$p = 73.52 - 482.04d + 3275.17d^2 - 11348.96d^3 + 18725.40d^4 - 11652.08d^5\ ,$$

where d is the mean grain diameter in millimeters.

A comparison of the McDaniel and Beebe formula predictions to Hamilton's values for sediments is shown in Table III-1. In Table III-2 we present the permeability calculated for Hamilton's sediment classes and also the relaxation frequency. In Figure III-2, we plot Hamilton's loss factor k_p for compressional waves on a log scale against the log of the ratio of porosity to permeability. This ratio is proportional to the relaxation frequency.

Table III-1. Comparison of McDaniel-Beebe fits with Hamilton empirical values for ρ_s and p.

Sediment Type	Mean Grain Diam. d (mm)	Mean Grain Diam. $M_z(\phi)$	Saturated Bulk Density ρ_s (g/cm^3) Hamilton	Saturated Bulk Density ρ_s (g/cm^3) McDaniel[a]	Porosity, p (%) Hamilton	Porosity, p (%) McDaniel[b]
Sand						
Coarse	0.5285	0.92	2.034	2.070	38.6	38.7
Fine	0.1593	2.65	1.941	1.920	45.6	44.8
Very fine	0.0960	3.38	1.856	1.857	50.0	48.9
Silty sand	0.0490	4.35	1.772	1.773	55.3	56.5
Sandy silt	0.0308	5.02	1.771	1.715	54.1	61.5
Silt	0.0237	5.40	1.740	1.682	56.3	63.8
Sand-silt-clay	0.0172	5.86	1.596	1.643	66.3	66.1
Clayey silt	0.0077	7.02	1.488	1.543	71.6	70.0
Silty clay	0.0027	8.52	1.421	1.413	75.9	72.2

[a] $\rho_s = 2.149 - 0.0864\ M_z$ g/cm^3

[b] $p(\%) = 73.52 - 482.04\ d + 3275.17\ d^2 - 11348.96\ d^3 + 18725.40\ d^4 - 11652.08\ d^5$, mm

Table III-2. Calculation of relaxation frequency, kHz.

Sediment Type	Mean Grain Diam. d (mm)	Mean Grain Diam. $M_z(\phi)$	Sorting σ_ϕ	Porosity % (McDaniel & Beebe)	Permeability (m^2) (McDaniel & Beebe)	Relaxation[a] Frequency, kHz $f_r = \frac{\beta\eta}{3\pi B_s}\times 10^{-3}$	Attentuation Rate k_p, dB/m/kHz (Hamilton)
Sand							
Coarse	0.5285	0.92	0.79	38.7	7.53×10^{-11}	0.545	0.48
Fine	0.1593	2.65	0.74	44.8	7.27×10^{-12}	6.541	0.51
Very fine	0.0960	3.38	0.98	48.9	1.95×10^{-12}	26.57	0.60
Silty sand	0.0490	4.35	1.29	56.5	3.36×10^{-13}	178.4	0.67
Sandy silt	0.0308	5.02	1.52	61.5	9.91×10^{-14}	657.81	0.64
Silt	0.0237	5.40	1.64	63.8	4.95×10^{-14}	1,367.7	0.57
Sand-silt-clay	0.0172	5.86	1.80	66.1	2.13×10^{-14}	3,292.7	0.12
Clayey silt	0.0077	7.02	2.20	70.0	2.53×10^{-15}	29,401	0.10
Silty clay	0.0027	8.52	2.73	72.2	1.58×10^{-16}	485,240	0.098

[a] Kinematic viscosity of fluid, $\eta = 1.0 \times 10^{-6}$ m^2/s

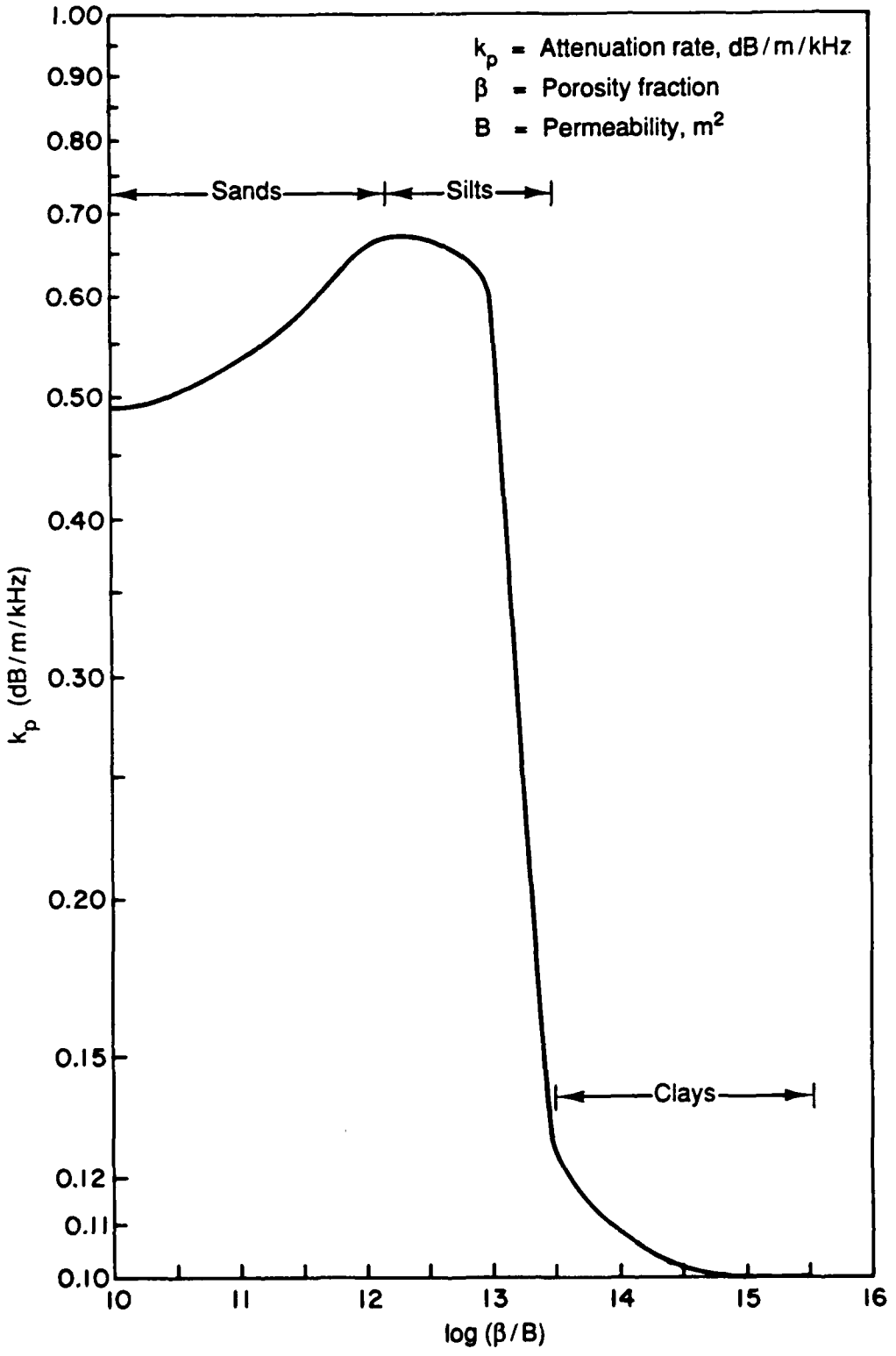

Fig. III-2. Sediment attenuation rate versus porosity/permeability ratio.

It can be seen from Figure III-2 that attenuations corresponding to ratios of porosity to permeability for silts and very fine sands behave entirely differently from those of clays. It can also be seen that the attenuation rate peaks for Biot theory relaxation frequencies corresponding to very fine sand and silts. This has been observed empirically by Hamilton[16] and confirmed semiempirically by Jensen and Kuperman[27] and by Akal and Jensen.[28] (See Table II-4, Section II.) This effect may be due to the frequency range of measurement.[35] Hamilton used a few kilohertz to tens of kilohertz just in the relaxation frequency range of silts and sands. (See Table III-2.)

4. Frequency Dependence of Attenuation Rate

As was seen in Figures II-3 and II-4 in Section II, Hamilton had adopted the convenient method of summarizing attenuation rate versus frequency measurements in terms of decibels per meter per kilohertz since he had found that in most cases at kilohertz frequencies the attenuation rate was proportional to frequency. Stoll[21,36] has been assembling data which show that there is a tendency away from this behavior for sands and silts at low frequencies. Figure III-3 is taken from a recent paper[36] where the attenuation predictions for sand and silt with properties listed in Table III-3 have been compared with recent measurement data.

Beebe *et al.*[37] present Figure III-4 showing sediment absorption using Biot theory, as a power law of frequency for various sediment types with mean grain sizes ranging from $M_z = 0.5\phi$ to 6.37ϕ.

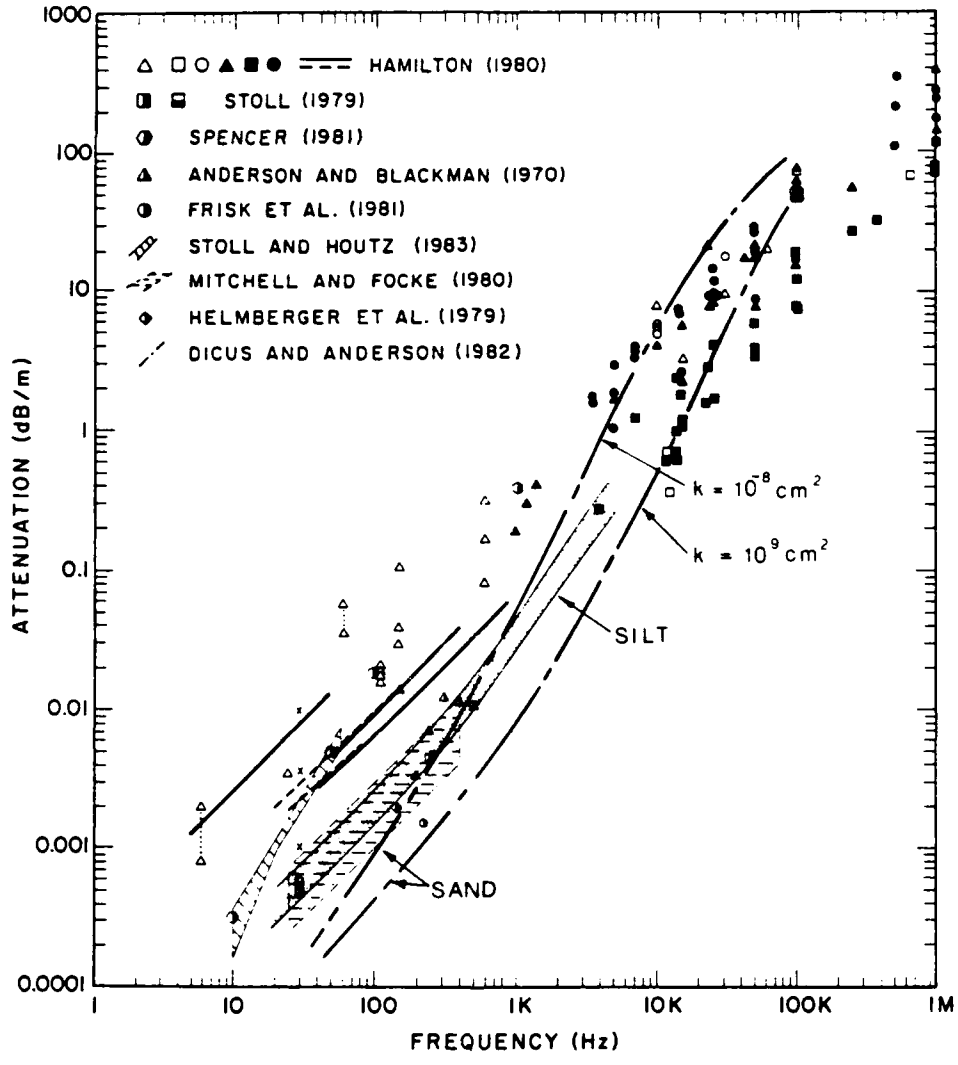

Fig. III-3. Laboratory and field data for attenuation versus frequency with curves showing predictions of Biot model superimposed. (Ref. 35)

Table III-3. Material properties used to calculate theoretical curves labeled "sand" and "silt" in Fig. III-3. (Ref. 36)

Input parameters	Sand	Silt
Bulk modulus of grains, K_r (Pa)	3.6×10^{10}	3.6×10^{10}
Bulk modulus of fluid, K_f (Pa)	2.0×10^{9}	2.0×10^{9}
Specific gravity of grains, ρ_r	2.65	2.65
Specific gravity of fluids, ρ_f	1.0	1.0
Shear modulus of frame, Re μ^* (Pa)	2.6×10^{7}	5.7×10^{7}
Bulk modulus of frame, Re K_b^* (Pa)	4.4×10^{7}	5.2×10^{7}
Logarithmic decrement of frame (shear)	0.04	0.075 to 0.148
Ratio of extensional to shear decrement, δ_E/δ_s	1.0	0.95 to 1.5
Porosity	0.4	0.5
Permeability, k (cm^2)	10^{-8} to 10^{-9}	2.5×10^{-10}

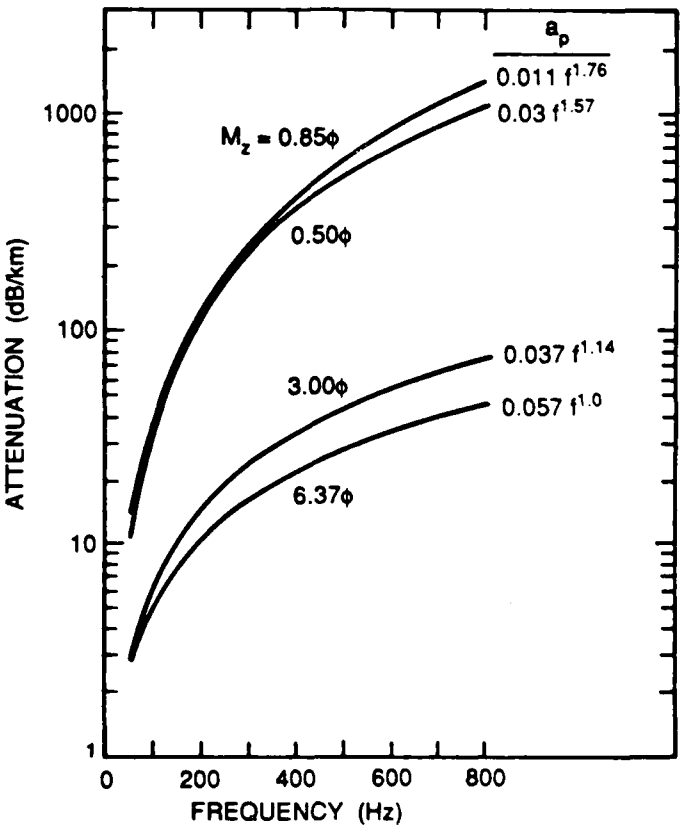

Fig. III-4. Predicted sediment absorption. (Ref. 37)

5. Dispersion

In studying acoustic propagation in shallow water, McDaniel and Beebe[31] also estimated sediment velocity using the Biot theory. As would be expected in the neighborhood of a relaxation process, they found that dispersion occurred for coarser sediments. Figure III-5 is their plot of predicted sediment velocity as a function of frequency and mean grain size. The velocities are somewhat lower than Hamilton's empirical estimates.[16] For finer sediments, $M_z \geq 4.0$, where no dispersion is predicted, the velocities are in agreement with Hamilton's empirical fits. Since small changes in the bulk

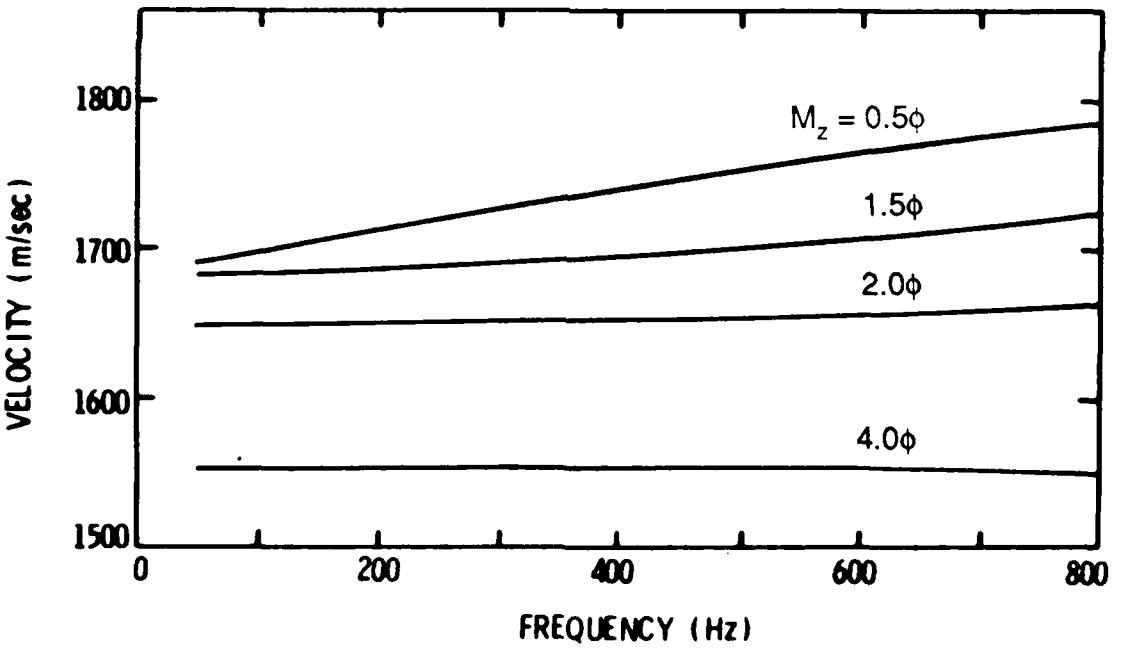

Fig. III-5. Predicted sediment velocity as a function of frequency and mean grain size. (Ref. 31)

modulus of the frame strongly affect the predicted sediment velocity, it is important to improve and expand the measurement of input parameters to the Biot model.

Finally, in Table III-4 we present values of the Biot parameters necessary to evaluate acoustic properties of sediments. Only two types of sediments are considered, "sand" and "soft sediment." The values in MKS units used by Yamamoto are also included for sand alone to show the range in values that different workers employ for the same sediment. It would appear that a more intense program of measurements is required to define sediments in terms of their Biot parameters.

Table III-4. Biot model material parameters frequently used.

Material Property	Stoll and Kan[61] and Stoll[21] Units	Sand	Soft Sediment	Beebe *et al.*[37] Units	(Daytona Beach) Sand	(Corpus Christi) Clay	Yamamoto[11] (MKS units)	Sand
Bulk modulus of grains, K_r	Pa	3.6×10^{10}	3.6×10^{10}	dyn/cm^2	5.6×10^{11}	3.8×10^{11}	Pa	3.6×10^{10}
Bulk modulus of fluid, K_f	Pa	2.0×10^{9}	2.0×10^{9}	dyn/cm^2	2.4×10^{10}	2.4×10^{10}	Pa	2.3×10^{9}
Density of grains ρ_r (g/cm^3)	g/cm^3	2.65	2.65	g/cm^3	2.71	2.67	kg/m^3	2.65×10^{3}
Density of fluid ρ_f (g/cm^3)	g/cm^3	1.0	1.0	g/cm^3	1.0	1.0	kg/m^3	1.0×10^{3}
Absolute viscosity of fluid, η	$\frac{dyn\cdot s}{cm^2}$	1.0×10^{-2}	1.0×10^{-2}	$\frac{dyn\cdot s}{cm^2}$	1.0×10^{-2}	1.0×10^{-2}	--	--
Kinematic viscosity of pore fluid	--	--	--	--	--	--	m^2/s	1.0×10^{-6}
Coefficient of permeability, k	cm^2	10^{-6} to 5×10^{-9}	1.6×10^{-11}	k, cm^2	7.5×10^{-7}	6.33×10^{-11}	k_z, m^2	1.0×10^{-10}
Pore size parameter, a_1	cm	6.7×10^{-3} to 6.7×10^{-4}	1.3×10^{-5}	cm	3.3×10^{-3}	3.08×10^{-5}	m	$a_1=\left(3\frac{k_z}{\beta}\right)^{1/2}$
Porosity, β	fraction	0.47	0.76	fraction	0.38	0.65	fraction	0.30
Rod velocity of frame, V_E	m/s	3.0×10^{2}	3.0×10^{2}	m/s	3.0×10^{2}	3.0×10^{2}	--	--
Shear velocity of frame, V_s	m/s	2.1×10^{2}	2.1×10^{2}	m/s	2.1×10^{2}	2.1×10^{2}	--	--
Log decrement for longitudinal vibrations of frame, δ_E	--	0.15	0.10	--	0.15	0.45	--	--
Log decrement for shear vibrations of frame, δ_s	--	0.15	0.10	--	0.20	0.60	--	--
Specific rod loss in frame, $\delta=\delta_E/\pi$	--	--	--		--	--	--	0.02
Specific shear loss in frame, $\delta=\delta_s/\pi$	--	--	--		--	--	--	0.02
Bulk modulus of frame, K_b	Pa	4.36×10^{7}	3.69×10^{7}	--	--	--	K_{SR}, Pa	$\frac{K_{SR}}{G}=[2n/(1-2n)+2/3]$
Shear modulus of frame, μ	Pa	2.61×10^{7}	2.21×10^{7}	--	--	--	G, Pa	5.0×10^{7}
Poisson's ratio of frame, n	--	--	--	--	--	--	N	0.333
Sediment bulk density, ρ	g/cm^3	$\rho=\beta\rho_f+(1-\beta)\rho_r$	--	g/cm^3	2.06	1.5	ρ, kg/m^3	$\rho=\beta\rho_f+(1-\beta)\rho_r$
Mean grain size M_z, (ϕ)	--	--	--	ϕ	0.85	6.37	--	
Sorting, $\sigma_\phi(\phi)$	--	--	--	ϕ	0.83	2.19	--	

IV. GEOACOUSTIC LAYER MODELS

1. Introduction

A geoacoustic model for the water and underlying bottom must be defined in order to obtain solutions of the acoustic wave equation. Boundary conditions must also be specified. A geoacoustic model must include the depth dependence of the density, compressional and shear wave velocities, and the corresponding attenuations in each sub-bottom layer to a depth that is dependent on the lowest frequency of interest. Shear and interface waves can be generated whenever a faster and harder layer is encountered. This process is accentuated at frequencies that are low enough to allow interaction with the semi-infinite basement.

Surficial sediments can be sampled with corers and grabs. Densities and grain sizes can be measured to estimate porosities, compressional and shear wave velocities, and attenuations. Photographs can also be taken to confirm the measured *in situ* environment. For deeper layers we must get information in other ways, such as historical and stratigraphic summaries or by seismic refraction analysis, dispersion analysis, and reflection profiling. Dispersion analysis provides a sensitive technique for determining the parameters of the uppermost bottom layers. Seismic refraction analysis is used to characterize the deeper subbottom layers. Subbottom seismic reflection profiling yields layer thicknesses. With special profiling techniques both surficial and subbottom layers can be classified.

2. Shallow Water Computer Models

If a realistic model of the water sound speed profile and the characteristics of the bottom and subbottom are obtained, there are a number of computer programs that can be used to solve the wave equation with appropriate boundary conditions. The solution methodology is based on either normal mode characterization,[38] the fast Fourier program solutions,[39] parabolic differential equation methods,[40] or ray approximations. Rough surfaces and sloping bottoms can also be accommodated in some cases. The parabolic differential equation solutions can also be used for range-dependent environments.

3. Geoacoustic Modeling

Tolstoy[41] was the first to introduce modern geoacoustic modeling when he extended the Pekeris two-fluid model to several layers. He performed a cw experiment in the frequency range 88-148 Hz in water 22.6 m deep south of Long Island. His geoacoustic model started with a geologic-sedimentary description and evolved into a three-layered liquid half-space with account being taken of locally measured attenuation coefficients. He emphasized the importance of determining the acoustical parameters of the various layers. As additional information for describing the geoacoustic model, he showed that minor changes may produce effects sufficient to destroy agreement between theory and experiment. The use of various criteria, particularly dispersion and mode-interaction wavelengths, is illustrated in this connection.

For a shallow-water layered-waveguide, he assumed that the upper boundary is a free surface and that all the layers are treated as fluids. This is a severe assumption, since some of the layers may be consolidated or semiconsolidated sediments. The nature of the lower boundary depends on several factors and its definition will demand, in each case, the exercise of some judgment.

He started by including, in all cases, the complete sedimentary column, and to consider it as lying on a semi-infinite elastic solid basement. In most cases this is too much detail and it is often possible to consider an incomplete sedimentary section lying over a semi-infinite fluid. Tolstoy found that a three-layered half-space was adequate for describing experimental conditions in this frequency range.

It is possible to find geographic areas, on the order of hundreds of square miles, for which no drastic changes take place in the bottom cross section. The layers and their boundaries are more or less horizontal and their sound velocities and densities remain relatively constant. The sediments can be treated as fluids for this purpose. The approximation is substantiated by the results of numerous refraction and dispersion studies.

The following quantities can be derived from easily performed experiments:

(a) Frequencies of the stationary values of group velocity U, especially of the Airy phase $U_{\min}$ of the first mode.

(b) The corresponding velocities, i.e., the numerical values of $U_{\min}$.

However, an Airy phase with a well-defined center frequency will have a poorly defined arrival time and vice versa.

(c) Continuous dispersion curves for transient excited modes.

(d) Mode interaction wavelengths $\Lambda_{m,n}$ for various frequencies and modes.

4. Geological and Oceanographic Models

Apparently, there can be a great variability in the geoacoustic specification of a single location, as well as its interpretation. For example, Matthews *et al.*[42] made a careful and detailed study and analysis of the Corpus Christi, Texas, area in which Rubano[43] of ARL/PSU had worked previously. They found that seasonal factors can enter the model specifications in terms of the water sound-speed profiles, bottom temperatures, and mud distribution thickness owing to wind conditions at the surface and also bottom currents. In defining the geoacoustic situation for future experimental design, they emphasized that a proper experiment will place the source and receivers in a waveguide composed of a water layer and a mud layer, with the lower waveguide boundary below the mud and defined by a significant impedance discontinuity. The depth to this discontinuity can be estimated to within ±1 m and the sound attenuation should increase one order of magnitude across this discontinuity. They also estimated that the sound attenuation rate (~ 0.06 dB/λ) should be lower than that used by Rubano in the same Corpus Christi site.

However, they claimed that sound attenuation is the geoacoustic parameter of lowest confidence and considered it to be an independent variable. Their future measurements will use inverse methods to define the bottom and subbottom acoustically at two frequencies, 50 Hz and 140 Hz, for comparison with their model.

Their geoacoustic model is shown in Table IV-1 which is obtained from the more detailed information of Table IV-2. They also show the Rubano model in Table IV-3 for comparison. They use the computer model of Ref. 44 for their propagation loss determinations.

Table IV-1. Geoacoustic model of Table IV-2 as modified for input to Acoustic Field Model SNAP. (Ref. 42)

Material	Depth (m)	Sound Speed (m/s)	Density (g/cc)	Sound Attenuation (dB/λ)
Sea surface				
	0.0	1544.7		
	10.0	1544.6		
Sea water	20.0	1540.8		
	30.0	1537.6	1.00	
Water-sediment				
	0.0	1517.6	1.56	0.06
Sediment	2.5	1512.0	1.56	0.06
	17.5	1537.6	1.56	0.06
Holocene-Pleistocene boundary				
Sediment half-space	17.5	1737.1	1.84	0.50

Table IV-2. Geoacoustic model for the ARL/PSU experimental site off Corpus Christi, Texas, (27°-31'N, 96°-58'W) predicted for August.

Material	Depth (m)	Sound Speed (m/s)	Density (g/cc)	Sound Attenuation (dB/m/kHz)
Sea surface				
	0.0	1544.70		
	2.5	1544.67		
	5.0	1544.47		
	7.5	1544.24		
Sea water	10.0	1544.57		
	12.5	1543.39		
	15.0	1542.53		
	20.0	1540.82		
	25.0	1539.13		
	30.0	1537.58	1.00	
Water-sediment interface				
	0.0	1517.6	1.56	0.030
	2.5	1512.0	1.56	0.034
	5.0	1515.3	1.56	0.038
Holocene silty clay	7.5	1518.5	1.57	0.042
	10.0	1521.8	1.57	0.046
	12.5	1525.0	1.58	0.050
	15.0	1528.3	1.58	0.054
	17.5	1531.5	1.58	0.058
Holocene-Pleistocene-boundary				
	17.51	1737.1	1.84	0.288
	20.0	1741.2	1.84	0.286
	22.5	1744.7	1.84	0.284
	25.0	1747.8	1.85	0.282
Late Wisconsin	27.5	1750.4	1.85	0.280
very fine sand	30.0	1752.8	1.85	0.277
	32.5	1755.0	1.86	0.275
	35.0	1757.0	1.86	0.274
	40.0	1760.0	1.86	0.270
	45.0	1763.0	1.87	0.266
Late Wisconsin	50.0	1766.3	1.87	0.263
parameters	55.0	1768.7	1.87	0.259
extended to	60.0	1770.9	1.87	0.256
approximate mid-	65.0	1772.9	1.88	0.253
and early	70.0	1775.4	1.88	0.250
Wisconsin	80.0	1780.4	1.88	0.244
sediments	90.0	1785.4	1.89	0.239
	100.0	1790.4	1.89	0.234

Table IV-3. Geoacoustic model for ARL/PSU experimental site, after Rubano (Ref. 43).

Material	Depth (m)	Sound Speed (m/s)	Density (g/cc)
Sea surface			
	0.0	1512.0	1.0
	30.5	1518.0	1.0
Water-sediment interface			
	0.0	1490.0	1.4
	4.0	1490.0	1.4
Sediment-sediment interface			
	4.0	1700.0	1.7
	35.0	1700.0	1.7
Sediment-half-space interface			
		1830.0	2.0

5. Geoacoustic Models — Local Variations

The importance of local variations in specifying geoacoustic models was studied by McDaniel and Beebe.[45] They found two constant depth sites, off Daytona Beach, Florida, with remarkably different attenuation rates for the first normal mode in the frequency range 40 to 800 Hz. The experimental equipment included:

- A vertical array of eight hydrophones, equally spaced.
- A bottom-mounted seismic receiver for refraction and shear velocity measurements. The sensor package consisted of two hydrophones and three mutually orthogonal geophones.
- Core and grab samples to derive absorption coefficients.

Seismic refraction and Stoneley wave measurements revealed that the seabed consisted of semiconsolidated sediment overlaid by a thin layer of sand. Compressional wave velocity for the semiconsolidated sediment layer was determined to be 2400 m/s and the shear wave velocity was estimated at 670 m/s. From modeling computations the differences in the measured low frequency loss could be accounted for by variations in the thickness of the surficial sand layer. Actual measurements of this thickness yielded a surficial layer of 5 m in one location as compared with 80 to 300 m previously reported.

6. Biot Theory Models

Matthews *et al.* use the Hamilton attenuation factor k_p, whereas McDaniel and her coworkers use Biot theory, to obtain values of attenuation coefficients and sediment velocities.

Sound speed in the semi-infinite half-space of Rubano's model was calculated from seismic refraction measurements. The depth to the half-space was calculated from the low frequency cutoff of the first mode (16 Hz). Rubano then used trial-and-error fitting of the group velocity dispersion data. Constant sound speeds were assumed for all layers in the Rubano model, except for the water profile.

In a series of papers,[31,37,45] McDaniel and her coworkers showed the consequences of using Biot theory in geoacoustic models to support the solution of the shallow water wave equation. They indicated that 16 parameters were needed for this purpose and

showed how to obtain their values for silty clay (Corpus Christi, Texas) and sand (Daytona Beach, Florida). They also derived empirical fits of permeability versus mean grain size and sorting (standard deviation) for this purpose. See Tables IV-4 through IV-6. Figure IV-1 shows their derived frequency power law of attenuation rate.

Yamamoto[11] has also shown how to solve the shallow water wave equation in terms of Biot theory and normal modes.

Table IV-4. Biot geoacoustic model input parameters. Universal parameters: $\rho_f = 1.0\ g/cm^3$, $k_f = 2.4 \times 10^{10}\ dyn/cm^2$, $\eta' = 0.01\ dyn \cdot s/cm^2$, $V_E = 3 \times 10^4\ cm/s$, $V_s = 2.1 \times 10^4\ cm/s$. *Site parameters are shown below. (Ref. 37)*

Site	M_z (phi)	σ_ϕ (phi)	k_r (dyn/cm²)	ρ_r (g/cm³)	ρ (g/cm³)	K (cm²)	a (cm)	α	β	δ_g	δ_s
Corpus Christi	6.37	2.19	3.8×10^{11}	2.67	1.5	6.33×10^{-11}	3.08×10^{-5}	3.0	0.65	0.45	0.60
Daytona Beach	0.85	0.83	5.6×10^{11}	2.71	2.06	7.5×10^{-7}	3.3×10^{-3}	1.25	0.38	0.15	0.20

Table IV-5. Geoacoustic model — Corpus Christi. (Ref. 37)

Layer		Depth (m)	Velocity (m/s)	ρ (g/cm³)	ϵ^a (dB/km)
1	(water surface)	0	1512	1.0	· · ·
		30.5	1518	1.0	· · ·
2	(interface)	30.5	1490	1.5	$0.057f$
		34.5	1490	1.5	
3		34.5	1700	1.7	$0.057f$
		65.5	1700	1.7	
4		65.5	1830	2.0	$0.057f$
		∞	1830	2.0	

[a]Frequency (f) in Hz.
[b]Shear effects were assumed negligible.

Table IV-6. Geoacoustic model — Daytona Beach. (Ref. 37)

Layer		Depth (m)	Velocity (m/s)	ρ (g/cm^3)	ϵ^a (dB/km)
1	(water surface)	0	1530	1.0	...
		32	1530	1.0	...
2	(interface)	32	1723	2.1	$0.011\ f^{1.76}$
		42	1723	2.1	
3		42	2222	2.2	$0.011 f^{1.76}$
		∞	2222	2.2	

[a]Frequency (f) in Hz.
[b]Shear effects were assumed negligible.

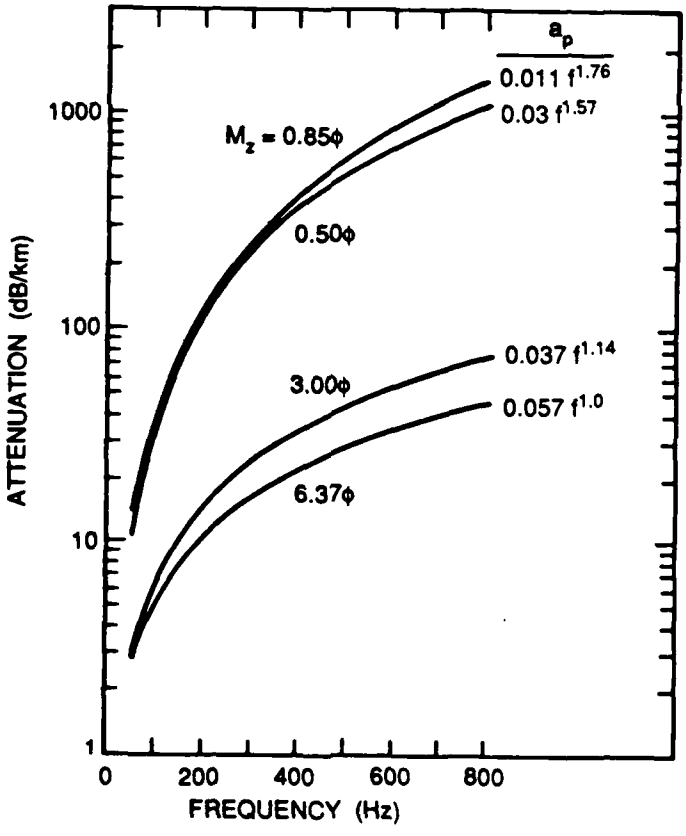

Fig. IV-1. Predicted sediment absorption versus frequency for various grain sizes, M_z (in φ–units). (Ref. 37)

7. Very Low Frequency Models

By "very low frequency" (VLF) we mean frequencies where the water layer is thin compared to a wavelength. In such cases, water and sediment layer characteristics may be combined into sound speed distributions down to the basement, where elastic solid boundary conditions are required.

For very low frequencies of 10 and 20 Hz, Tolstoy[46] treated the geoacoustic model as a point source imbedded in a thick sedimentary layer (607 m) overlying a solid elastic basement of Poisson ratio 1/4. The sediment itself was treated as a fluid with sound velocity varying with depth according to the form $(pz+q)^{-1/2}$. The wave equation was solved by numerical integration. In addition, he treated the coupling effects between the sediment layer and the basement, including Stoneley interface waves.

To test his modeling procedure at low frequency, Tolstoy[46] made 10 and 20 Hz cw measurements at the same location, Fire Island, where he previously studied cw modeling in the frequency range 88-150 Hz. He treated a heterogeneously layered sedimentary column, with continuous variation of compressional velocity with depth, as a fluid (see Figure IV-2). The law of velocity variation was chosen for the numerical integration solution to the wave equation for convenience, rather than as a best fit to velocity data. He concluded that an interface between sediment layers is less severe for long wavelengths and that the standard interpretation of refraction profiles may often give sharp boundaries when actually there are only increases in the velocity gradient. He also

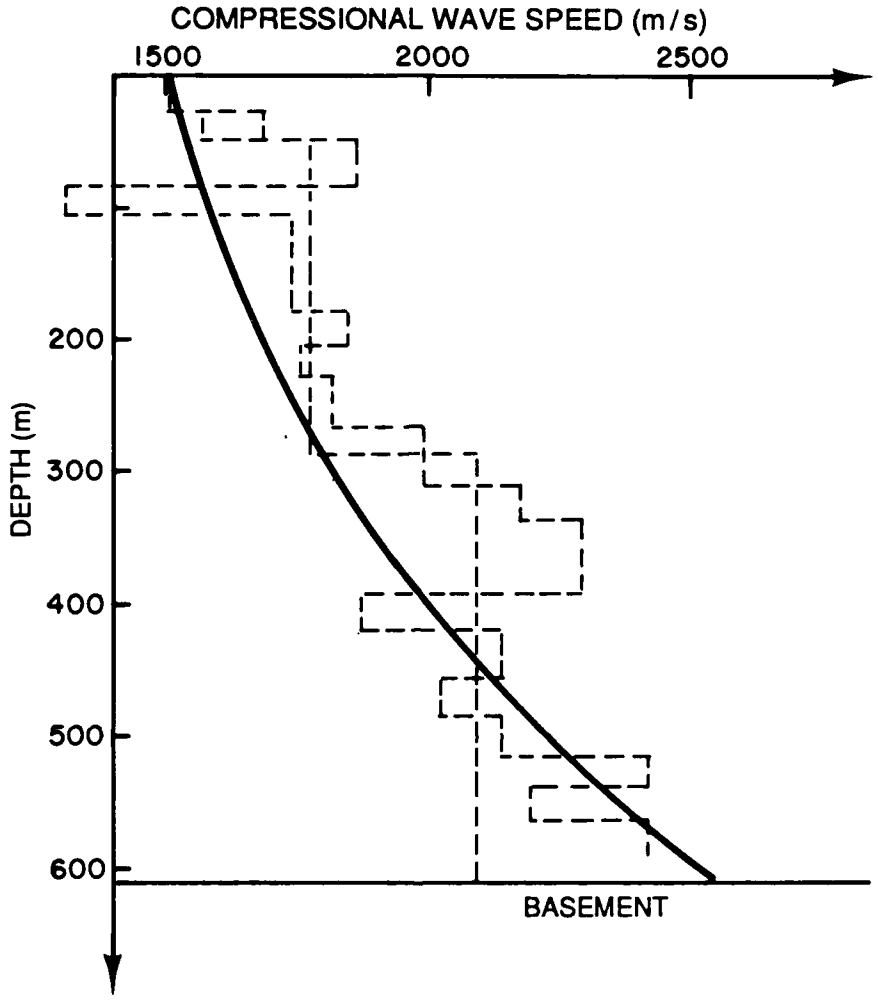

Fig. IV-2. Real and assumed cross sections at location of experiment. The indicated layers were determined by various measurement methods. The solid line represents the analytical expression used to represent the measurements. See Ref. 46 for more details. (Ref. 46)

reasoned that the determination of the velocity of compressional waves at the bottom of the sediment column was not very reliable.

The number of modes involved at VLF for propagation in the sediments is much larger than in the 88-150 Hz experiment, where agreement was obtained for situations

involving at most four modes. Even in the latter case some effort was required to obtain a more accurate theoretical model than the one given by seismic information alone. At 10 and 20 Hz, as many as 11 modes are involved in a crudely oversimplified model.

Although he found that the measured and computed sound fields agreed in the range from 1 to 5 km, he felt that the measured results and the theory could be brought closer together by introducing a few boundaries between sediments to obtain a more realistic velocity distribution in depth. He also felt that at least part of the sedimentary cover should be treated as an elastic solid.

Although progress is being made in modeling observed field data in moderately unstratified media, it is often incorrect to assume a laterally stratified medium in estimating propagation loss because of oceanographic and geological complexity. Such is the case for the Scotian shelf area, which is a specific shallow water environment. It is important to study the acoustics of such areas as well.

Brocher *et al.*[47] made explosive source measurements on a shallow sandy bottom in 67 m of water on the Scotian shelf at very low frequencies from 5 to 40 Hz. They used OBSs (ocean bottom seismometers) and sources near the nominal cutoff frequency (5 Hz). They were able to compare received signals as a function of frequency, source depth, azimuth, and mode of propagation. As expected, they found that propagation loss rates depended on azimuth and range. Lateral inhomogeneity in the acoustic path caused propagation loss just below the cutoff (5 Hz) to be about the same as above the cutoff

(≥10 Hz). This was attributed to two possible causes: (1) the sediment attenuation was fairly constant in this frequency range or (2) mode coupling, owing to the range-dependent acoustic environment, was relatively efficient near cutoff.

They also found that nearly all losses arose from the sediment attenuation of compressional waves, and that scattering and conversion to shear waves, and generation of interface waves, were relatively unimportant. Also, a loss rate minimum at 20 Hz existed on the shelf.

The geoacoustic environment was further defined by use of the refraction and interface wave dispersion data, as well as existing geological data. The shelf in the study area is covered by a thin veneer (0-15 m) of Pleistocene Sable Island sand and gravel. The surficial sediment on this portion of the shelf is a sand facies containing less than 50% gravel. The sand varies from finegrained to coarsegrained (0.2 to 5.0 mm) and is well sorted. The bedrock in the study area is not known. It could be underlain by either Quaternary glacial till or by Tertiary or Mesozoic bedrock. Available echograms lack the penetration necessary to map this deeper structure. However, the Scholte wave dispersion data suggest that the underlying sediments are more consolidated than typical Quaternary glacial deposits.

In their geoacoustic modeling, they again use a three-layer model consisting of ocean layer, sediment layer, and sediment half-space (see Figure IV-3, Table IV-7, and Figure IV-4).

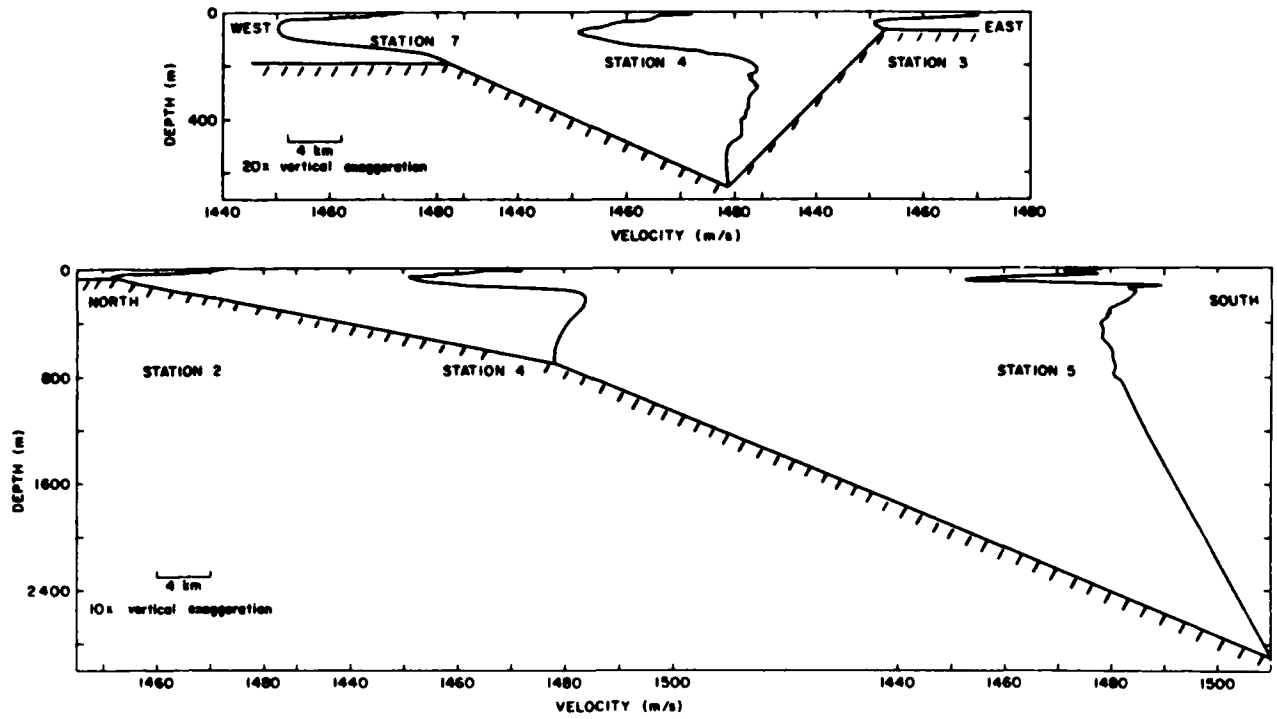

Fig. IV-3. Sound velocities along (top diagram) and perpendicular to (bottom diagram) the slope. Note that all of the Scotian shelf and much of the slope is bottom limited. (Ref. 47)

Table IV-7. Near seafloor velocity — density structure. (Ref. 47)

Density (g/cm³)	v_s (m/s)	v_p (m/s)	Thickness west of the transition (m)	Thickness east of the transition (m)
1.0	0	1500	67	67
1.7	262	1550	22	0–6
1.8	520	1600	Half-space	Half-space

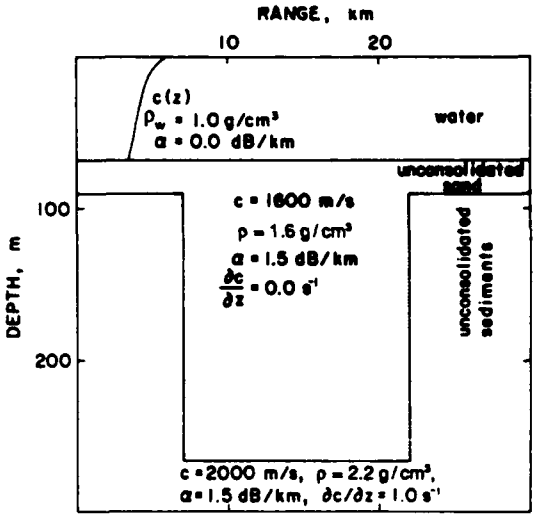

Fig. IV-4.
Geoacoustic model used in the parabolic equation approximation calculation. The vertical exaggeration in this figure is 100:1. The actual bathymetry used to calculate the loss rates is not shown in this figure. (Ref. 37)

V. REFLECTION OF PLANE WAVES BY SEDIMENTS

1. General

Many workers have studied the theoretical characteristics of the plane wave reflection coefficient based on various geoacoustic models of the water, seabed, and sub-bottom. They examine bottom loss versus the angle of incidence and frequency, and attempt to identify the mechanisms at work. Angles with little or large loss, or rates of change of loss, are considered in determining propagation loss versus range and transducer depth. The models usually consider water overlying one or two sediment layers plus a basement. Our ability to calculate expected model behavior has outstripped our ability to specify a model uniquely. We require improved knowledge of the appropriate sedimentary properties and the ability to measure these properties.

Important bottom properties at low frequencies between 20 Hz and 500 Hz include water depth, compressional wave speed and attenuation, sediment depth to the basement, and wave speeds and attenuations in all the sedimentary strata. Other physical properties are: density, porosity, mean grain size and its sorting, pore pressure, permeability, rigidity, and their depth dependence. Quantities that relate to attenuation in sediments are: the quality factor Q, the amplitude attenuation rate α (Np/m), and the log decrement δ. Here, $\frac{\pi}{Q} = \delta = \frac{\alpha V}{f}$, where V is the compressional sound speed in m/s and f is the frequency in Hz. To convert α in Np/m to the intensity attenuation rate a in dB/m, we

multiply α by 8.686. Yamamoto has found it quite useful to work with the quantity 1/Q. Instead of using the logarithmic decrement δ, he uses "specific loss" which is δ_E/π or δ_S/π for rod or shear vibration losses.

2. Fluid-Fluid Model

The Morse-Mackenzie[5] expressions for acoustic reflection from the sea bottom are based on a lossy two-fluid model. In using this model it has now become customary to use sediment characteristics specified by Hamilton.[16] The sediment is modeled as a deep homogeneous layer with density and sound speed specified with respect to seawater. An attenuation coefficient is also used that is assumed to be proportional to frequency and is obtained from the sediment porosity or the mean grain size correlations. On this basis, the reflection coefficient is found to be independent of frequency, and there is no critical angle in the true sense.

If the homogeneous lossy sediment fluid layer is thin enough, and underlain by a rigid basement, then it has been shown[48,49] that large fluctuations in the reflection coefficient can be obtained as the angle of incidence is changed. Note that the angle of incidence is the complement of the grazing angle.

3. Sediment Layer with Rigidity

A more realistic approach to understanding and applying the acoustics of sediments is to include the effect of rigidity. Here, the development of the subject may be

approached in several steps. First, we assume a homogeneous sediment layer with rigidity and consider the generation of shear waves as well as compressional wave transmission. Next we expand our view by considering the effect of depth on wave velocities and attenuations. After this treatment would come an examination of smooth anisotropic layering in the sediment. Finally, the effects of discontinuous anisotropic layering would be treated.

For small values of rigidity, a compressional wave entering the sediment can generate shear waves whose main effect would be to act as a sink for compressional wave energy. Bucker *et al*.[12] have shown that if the Stoneley-Scholte interface wave velocity and attenuation can be measured, then the velocity of the shear waves can be calculated from expressions by Strick and Ginzbarg.[50]

Hastrup[49] finds that the bottom-reflection loss from a hard bottom near grazing incidence, or from one that has a hard subbottom, can, in certain cases, be fairly high. This can result in higher propagation losses in shallow water than usually expected. Two frequently observed cases have been studied: (1) where the bottom can propagate shear waves and, (2) where the hard subbottom is covered by a layer of soft unconsolidated sediments. The first case causes a relatively large low-frequency attenuation resulting in a higher optimum frequency for propagation. The second case results in poor propagation for selected frequencies.

For viscoelastic bottoms, the acoustic properties are defined by the compressional and shear wave velocities, the attenuation factors associated with these waves, and the material density. Akal and Jensen[28] make the point that shear rigidity is a fundamental property of ocean-bottom sediments and must be included in a realistic model of the seabed. In simple bottom models, based on viscoelastic theory, shear properties are often neglected. This can be justified only for very "soft" sediments like clayey silt in which the shear velocities are low, i.e., $\leq$ 200 m/s. In harder, unconsolidated sediments, shear properties are very important and might even dominate the reflection behavior. The existence of interface waves in the seafloor is intrinsically related to the shear properties of the bottom material.

Akal and Jensen have also computed reflection loss versus grazing angle for different bottom types with the bottom material properties of Table V-1. They used the model developed by Hastrup [49] and the results are shown in Figure V-1. See also Table II-4.

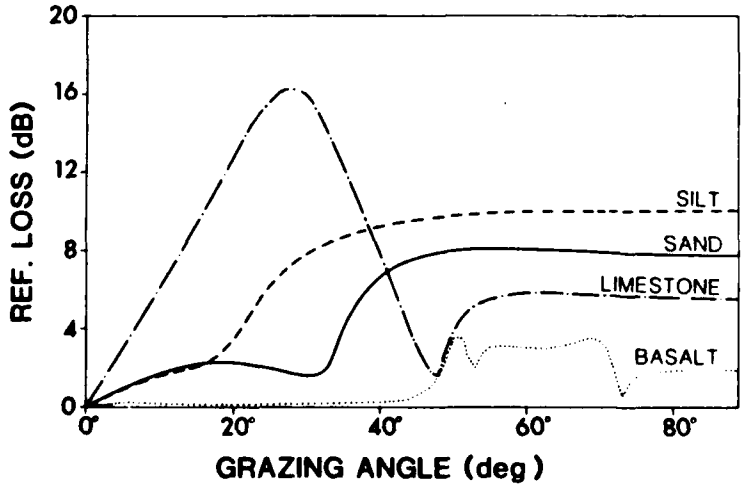

Fig. V-1.
Computed reflection loss versus grazing angle for different bottom types. (Ref. 28)

Table V-1. Geoacoustic parameters for different bottom types. (Ref. 28)

Bottom Type	Density (g/cm^3)	Compress. speed (m/s)	Shear speed (m/s)	Compress. attenuation (dB/λ_p)	Shear attenuation (dB/λ_s)
SILT	1.8	1600	200	1.0	2.0
SAND	2.0	1800	600	0.7	1.5
LIMESTONE	2.2	2250	1000	0.4	1.0
BASALT	2.6	5250	2500	0.2	0.5

4. Reflectivity of the Ocean Bottom at Low Frequency -- Shear Wave Effects

The plane wave reflection coefficient is particularly useful in investigating the influence of sediment parameters on bottom reflection loss.[51–54] Most models of the bottom are taken as fluid sediment. Hawker and Foreman[55] have integrated the wave equation numerically for fluid sediments and can treat sediments with arbitrary depth variations. This approach can include solid sediments, and recent work has concentrated more on the characteristics of solid sediments or sediments with rigidity. Bucker *et al.*[12] and Fryer[56] use the Thomson-Haskell[57,58] matrix approach in their models for which the depth variation of the sediment parameters is treated as a series of homogeneous layers.

Working with a hypothetical turbidite section in deep water, Fryer[56] has found that, when the elastic parameters of the sediment vary continuously with depth, the conversion of compressional wave energy to shear wave energy is unimportant at frequencies above 20 Hz. However, conversion to shear energy does occur at sediment discontinuities. This strongly affects reflectivity at all frequencies between 0.1 and 100 Hz, except for small grazing angles and near-normal incidence.

Vidmar and Foreman[59] present a method for computing the complex plane wave reflection coefficient of an acoustic wave impinging on an ocean bottom consisting of a single inhomogeneous (fluid or solid) sediment layer overlying a semi-infinite homogeneous (fluid or solid) substrate. Within the sediment layer, the density, compressional wave speed and attenuation and the shear wave velocity and attenuation can vary arbitrarily and independently. A matrix formulation is used in which depth-separated wave equations are replaced by a "propagator" matrix. The elements of the propagator are calculated by numerical integration of the Helmholtz equations with depth-dependent wave numbers. The propagator formalism[60] replaces the differential equations describing shear and compressional wave propagation by a matrix that relates boundary values at the top and bottom of the layer. The model is unique in that elements of the propagator matrix are calculated by direct numerical integration of the depth-separated wave equations for both compressional and shear waves. Direct numerical integration permits arbitrary depth variations of sediment parameters to be treated without recourse to approximation by homogeneous layering or special functions.

Figures V-2 and V-3 show their geophysical model while Table V-2 gives actual values for the parameters. Figures V-4 and V-5 show the results at 20 Hz for two different turbidite layer thicknesses, 518 m and 36 m. Whereas the plane wave reflection coefficients for the solid and fluid models of the thick section agree well, except for grazing angles between 50° and 70°, there are remarkable differences for the thin layer up to about a 70° grazing angle.

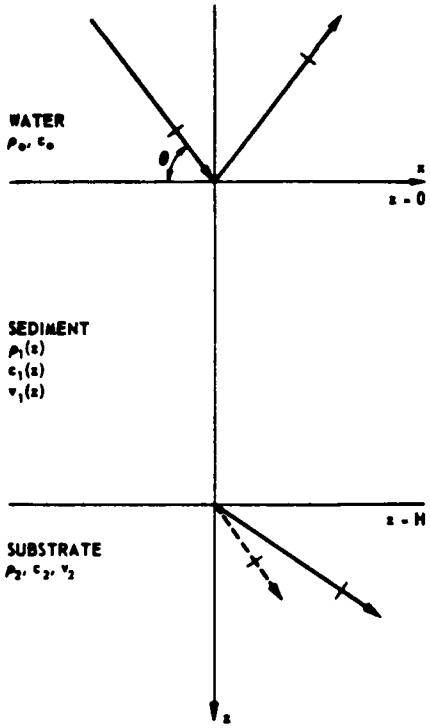

Fig. V-2.
The physical model. (Ref. 59)

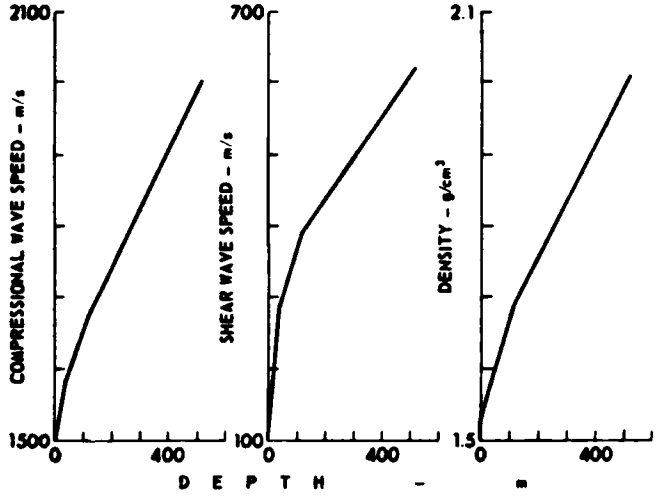

Fig. V-3.
Parameters of the hypothetical turbidite layer. (Ref. 59)

Table V-2. Physical parameters of sediment studied. The attenuations are given for a frequency of 20 Hz. (Ref. 59)

Depth (m)	c_0 m/s	v_0 m/s	ρ g/cm³	α_p dB/m	α_s dB/m
Water	1530	···	1.03	···	···
0	1510	116	1.53	0.001 3	0.169
36	1582	283	1.579	0.002 0	0.112
120	1674	391	1.689	0.004 0	0.172
518	1992	621	2.010	0.002 7	0.087
Substrate	4460	2400	2.46	0.000 16	0.000 79

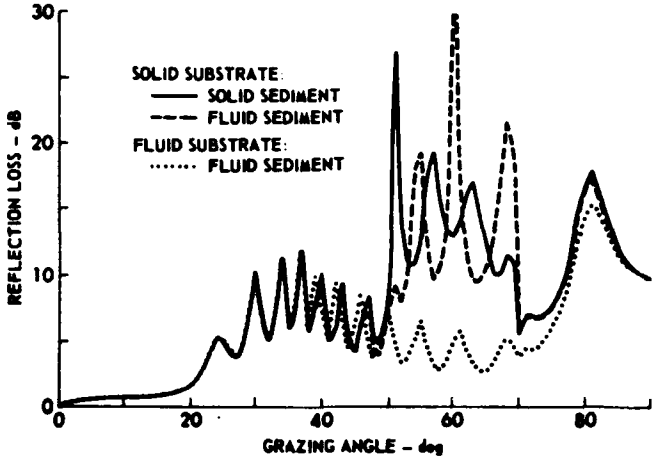

Fig. V-4.
Reflection loss versus grazing angle for a 518-m-thick hypothetical turbidite layer at 20 Hz. (Ref. 59)

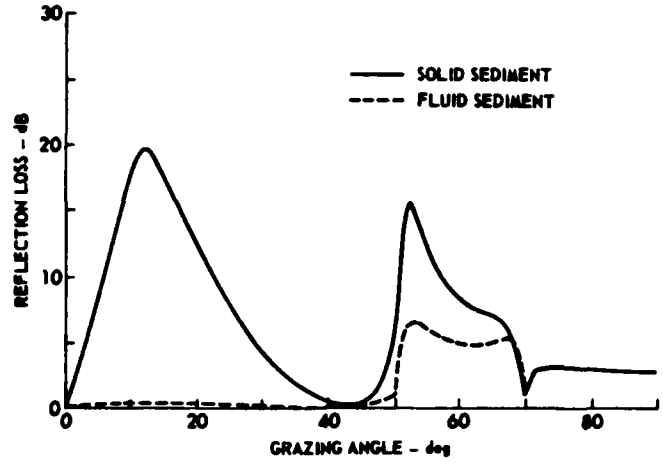

Fig. V-5.
Reflection loss versus grazing angle for a 36-m-thick hypothetical turbidite layer at 20 Hz. (Ref. 59)

5. Biot Theory and Plane Wave Reflection Coefficients

Stoll and Kan[61] have studied the reflection and transmission properties of a water-sediment interface where the sediment is modeled as a poroviscoelastic half-space. The model predicts attenuation and wave velocity on the basis of parameters that are related to porosity, grain size, permeability, and effective stress. Energy losses in the skeletal

frame of the sediment, as well as viscous losses in the pore water-frame interactions, result in an overall attenuation that is a nonlinear function of frequency.

Biot's theory of wave propagation in a poroviscoelastic medium predicts that three kinds of waves can propagate in the sediment. Two are compressional waves and the third is a shear wave. The compressional wave of the first kind is similar to the usual compressional wave in elastic theory. It attenuates slowly and propagates with very little dispersion except at the relaxation frequency. The other compressional wave is a form of diffusion wave that attenuates very rapidly and travels at a much lower velocity. For this wave, the motion of the fluid is out of phase with the skeletal frame, whereas in the first compressional wave they are nearly in phase.

In the following discussion, homogeneous plane waves in the water may be incident at all angles to a half-space composed of a porous sediment. The phase velocity and attenuation in the sediment depend on the material properties of the sediment and on the angle of incidence of the generating wave. The theory is applied to models of a sand bottom and a soft sediment bottom of high porosity. The physical properties chosen for the examples are summarized in Table V-3.

The magnitude of the amplitude reflection coefficient versus the angle of incidence is plotted in Figure V-6 at different values of permeability for a sand bottom of porosity 0.47 and a frequency of 10 kHz. Stoll and Kan distinguish between lossy fluid and frame

Table V-3. Material properties for examples. (Ref. 61)

	Sand (fine sand)	Soft sediment (silty clay)
Bulk modulus of grains, K_r (Pa)	3.6×10^{10}	3.6×10^{10}
Bulk modulus of fluid, K_f (Pa)	2.0×10^{9}	2.0×10^{9}
Specific gravity of grains, γ_r	2.65	2.65
Specific gravity of fluid, γ_f	1.0	1.0
Shear modulus of frame, μ (Pa)	2.61×10^{7}	2.21×10^{7}
Bulk modulus of frame, K_b (Pa)	4.36×10^{7}	3.69×10^{7}
Log decrement of frame (shear)	0.15	0.5
Log decrement of frame (dilatation)	0.15	0.5
Porosity	0.47	0.76
Permeability (specific) k (cm^2)[a]	10^{-6} to 5×10^{-9}	1.6×10^{-11}
k (m^2)	10^{-10} to 5×10^{-13}	1.6×10^{-15}

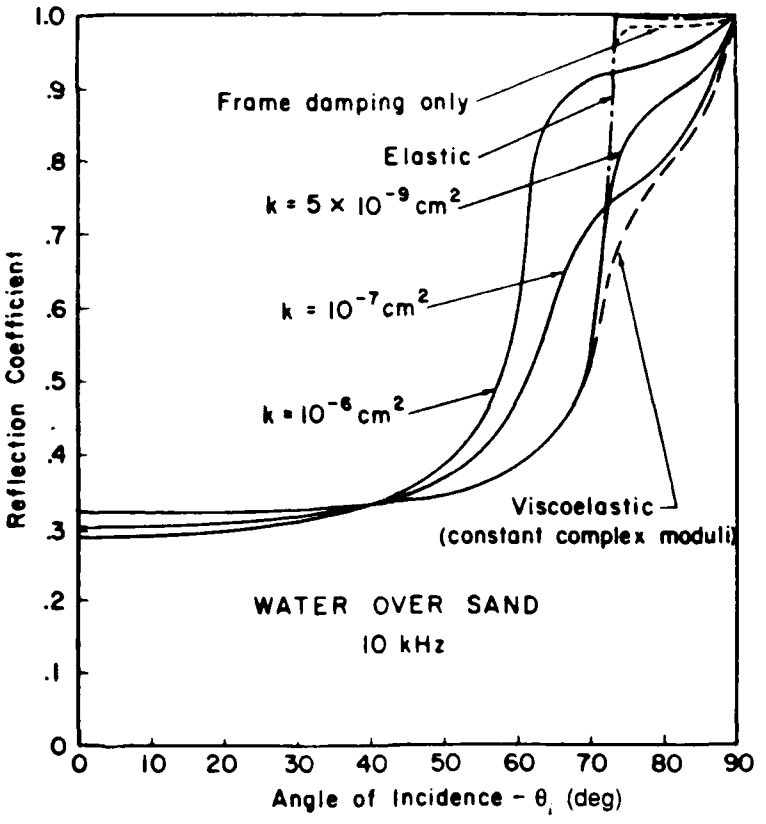

Fig. V-6. Amplitude reflection coefficients, A_r/A_i, for water over sand at 10 kHz. In this figure, k = specific permeability. (Ref. 61)

models and viscoelastic models by noting the important effects of permeability. In fact, Figure V-7 shows that frequency has about the same effect as permeability. A factor of ten in permeability produces the same effect as a factor of ten in frequency.

Figures V-7 and V-8 show the effect of frequency on the amplitude reflection coefficient for the same model of clean sand. Below 100 Hz the properties of the skeletal frame are important and the viscous losses somewhat less significant. As the frequency increases, the fluid losses begin to control the overall attenuation and the response is

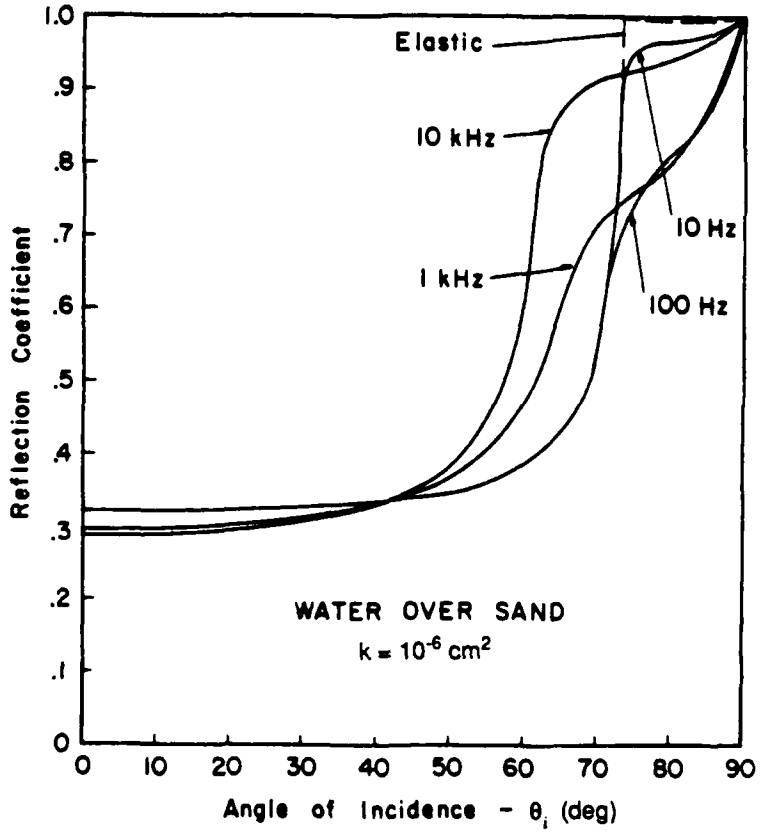

Fig. V-7. Amplitude reflection coefficients, A_r/A_i, for water over sand at all angles of incidence for different frequencies. (Ref. 61)

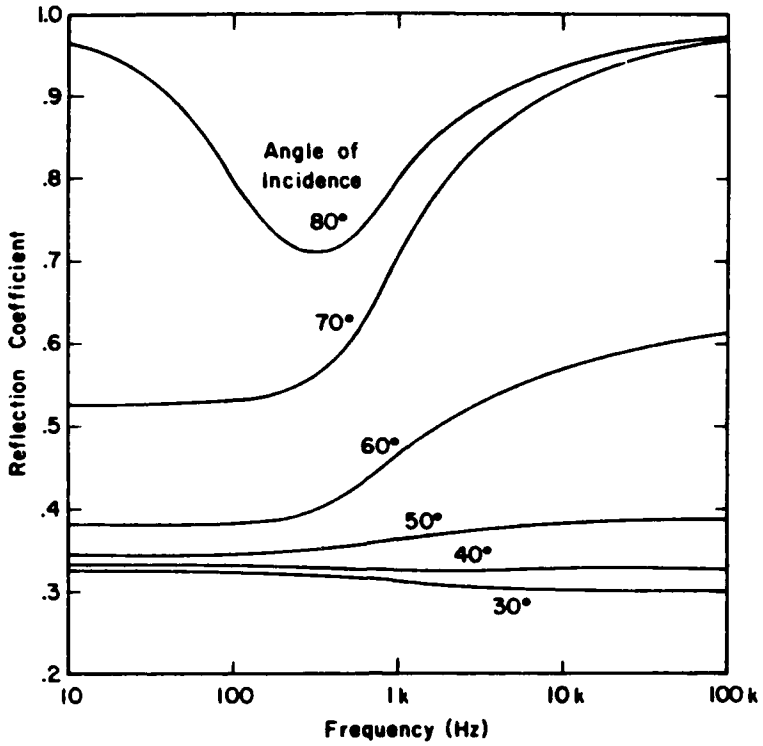

Fig. V-8. Amplitude reflection coefficients, A_r/A_i, for water over sand at all frequencies for several different angles of incidence. (Ref. 61)

significantly different. The reflection coefficients begin to deviate from the elastic case at angles well below the critical angle and the marked dependence on frequency is evident. Thus at certain angles of incidence, the reflection coefficient becomes strongly dependent on frequency and the interface should act as a filter with respect to broadband energy.

A comparison of Figures V-6 and V-7 shows that there is essentially an equivalent relationship between permeability and frequency as pointed out in Section III. This

equivalency is useful in visualizing the effects of fluid mobility. In the low frequency range of ten hertz to several hundred hertz, which occurs in marine seismology when an airgun source is used, the model suggests that there will be a marked difference between an ordinary viscoelastic model and a poroviscoelastic model only when a sand or silt layer of high permeability is encountered. In the high kilohertz range, the effects of fluid mobility (permeability) may be significant in a wider variety of marine sediments.

The difference between the angle of refraction for an elastic and a poroviscoelastic material is shown in Figure V-9. There is no "critical angle" for the poroviscoelastic

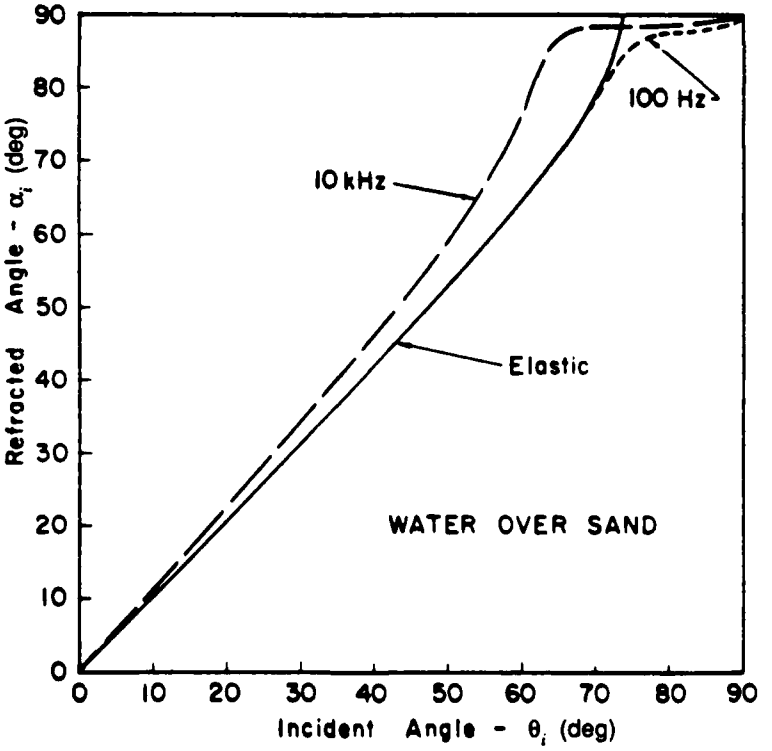

Fig. V-9. Incident angle versus refracted angle for elastic and porous, viscoelastic cases. (Ref. 61)

case. For the case shown, less than 1% of the total energy is converted to either shear or compressional waves of the second kind. Moreover, the velocity of shear waves is very low (118 m/s at 100 Hz) so that there is no critical angle with respect to incipient shear waves. Dispersion curves (velocity versus frequency) for the sediment model used in this example have been presented elsewhere.[62]

By neglecting the viscous losses in the model, the attenuation expressed as a logarithmic decrement is about 0.02 at all frequencies. This is much too low, except at very low frequencies, so the importance of viscous losses becomes obvious. On the other hand, Figure V-6 shows that, for many sediments of low permeability, the simple viscoelastic model is a satisfactory approximation.

Figure V-10 shows a plot of both the reflection and refraction coefficients for a soft sediment of high porosity and low permeability. For this case the velocity of the compressional wave of the first kind is somewhat less than the velocity of the water wave and there is an angle of intromission. At 100 Hz the velocity of the compressional wave of the first kind is 1377 m/s. For this situation the curves for the general model are just about the same as for the elastic case.

In summary, for the general case where viscous losses in a saturated sediment are important, the reflection coefficient is frequency dependent at angles well below the conventional critical angle of an elastic solid. This may occur at low frequencies in sedi-

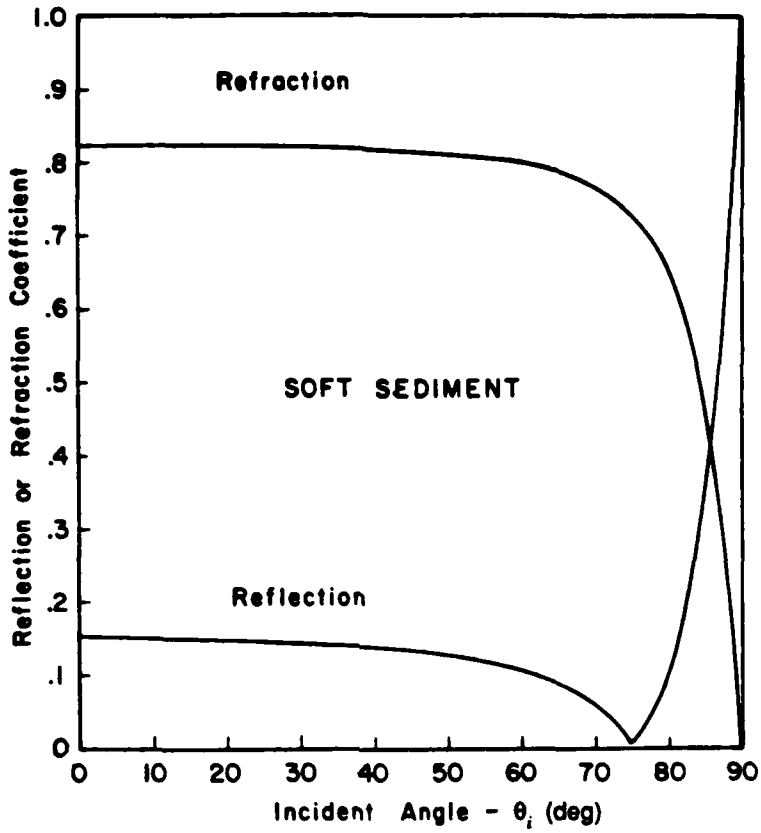

Fig. V-10. Amplitude reflection and refraction coefficients for water over soft sediment. (Ref. 61)

ments of high permeability or at high frequencies in sediments of lower permeability. This angular dependence is important in designing experiments using the frequency filtering effect of a water-sediment interface.

6. Stoneley Waves and Plane Wave Reflection Coefficients

Hawker[53] considers a single inhomogeneous fluid layer (clay) overlying a semi-infinite solid substrate (basalt) and the effects of Stoneley waves on plane wave reflection loss. This model is broadly characteristic of large areas of the North Pacific Ocean.

Hawker shows that there is a mechanism operating which causes a large and apparently anomalous increase in loss at low grazing angles. He considers various sediment layer thicknesses and sediment types as well as several different frequencies. He then examines the reflection coefficient for a geoacoustic model consisting of an inhomogeneous layer (nonzero sound speed gradient) overlying a homogeneous solid substrate basement. He finds peaks in the loss at low grazing angles that are independent of the frequency and that are related to the shear wave speed and attenuation in the substrate.

The fact that the location of the loss peak (about 17°) is nearly independent of frequency indicates the presence of an interface wave of the Stoneley type. In homogeneous media, Stoneley waves have a phase velocity that is independent of frequency. The peak location is sensitive to layer thickness and sediment type.

For certain configurations of layered fluids overlying a solid substrate, the reflection loss displays narrow peaks of significant amplitude. Hawker[54] extends the classical theory of Stoneley waves to inhomogeneous media and shows that the angles at which reflection-loss peaks occur are precisely those angles for which the horizontal component of phase velocity in the fluid sediment equals the Stoneley wave phase velocity. With this theory he can also explain the near independence of the reflection loss peaks on frequency.

VI. PROPAGATION LOSS AND OPTIMUM FREQUENCY

1. Introduction

The objective of studying plane wave reflection coefficients is to develop information from their grazing angle and frequency dependence to infer the acoustic properties of the sediment and basement. A second objective is to use the information to calculate the propagation loss in the water as a function of the range and the depth of transducers.

The use of the optimum propagation frequency is becoming standard for estimating bottom sediment effects and consequent modeling; however, Jensen and Kuperman[27] that the depth of the water is the most important factor. In this section we consider the effects and relative importance of three sediment parameters at low frequencies. The three parameters are: (1) permeability, (2) compressional wave attenuation in the sediment, including frame loss, and (3) rigidity or shear modulus.

In the frequency range of 20 to 500 Hz, geoacoustic layering must be combined with the sediment parameter effects in deducing loss characteristics of the seabed. In general, the estimation of optimum frequencies, in the sense of minimum loss at a given range or longest range for a given frequency, should not be based on the presence of only a single layer of homogeneous viscoelastic sediment. A layer of silty clay overlying a harder sand bottom will have the effect of deepening the shallow water channel and lowering the optimum frequency. The case is different, of course, for a consolidated sediment or bedrock bottom.

2. Permeability Effects

Akal[63] found that the optimum frequency varied inversely with porosity. For 100 m of water over a sand bottom, the optimum frequency was about 250 Hz, and over a clay bottom it was 50 Hz. Akal's figure (Figure VI-1) shows optimum frequency as a function of bottom type and relative sound speed for two water depths, 60 and 120 m. The deeper the water, the lower the optimum frequency for a given bottom type. Rubano[43] also found an optimum frequency of about 50 Hz for shallow water off Corpus Christi, Texas. Here there was a layer of silty clay, which Rubano estimated to be about 4 m thick, that was underlain both by a layer of silty sand 31 m thick and an infinite half-space of coarse sand. The depth of the water was 30.5 m. These sediment layer depths were determined by refraction shooting and dispersion analysis.

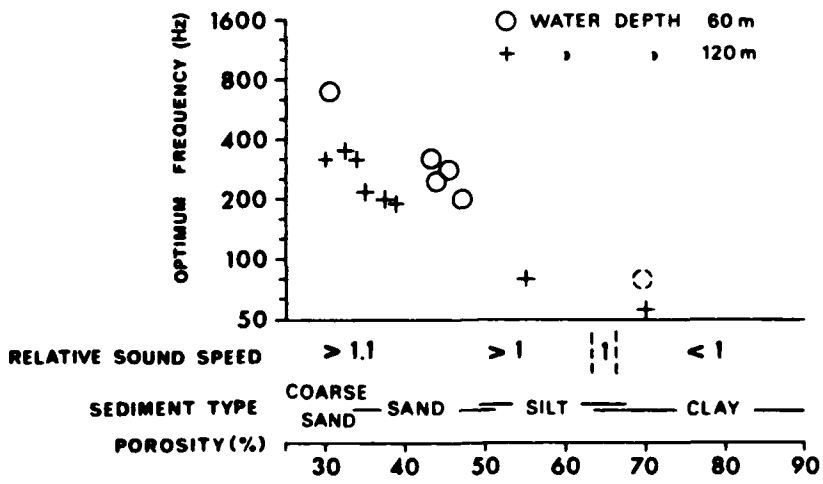

Fig. VI-1. The dependence of optimum propagation frequency on sea floor characteristics. (Ref. 63)

At this point, we include a figure (Figure VI-2) from a paper by Rubano's colleagues, McDaniel and Beebe,[31] which summarizes Rubano's results and relates them to other types of sedimentary covers. McDaniel and Beebe point out the importance of flow permeability for determining sediment attenuation rates and therefrom optimum transmission frequencies for given geoacoustic models. We have previously shown their semiempirical expression for permeability as a function of the mean grain size and sorting. Sorting is the standard deviation of the grain size distribution, σ_ϕ. For fine sediments, a knowledge of the acoustic characteristics of deeper strata is needed to predict transmission losses. The large low-frequency losses obtained for the coarser sediments

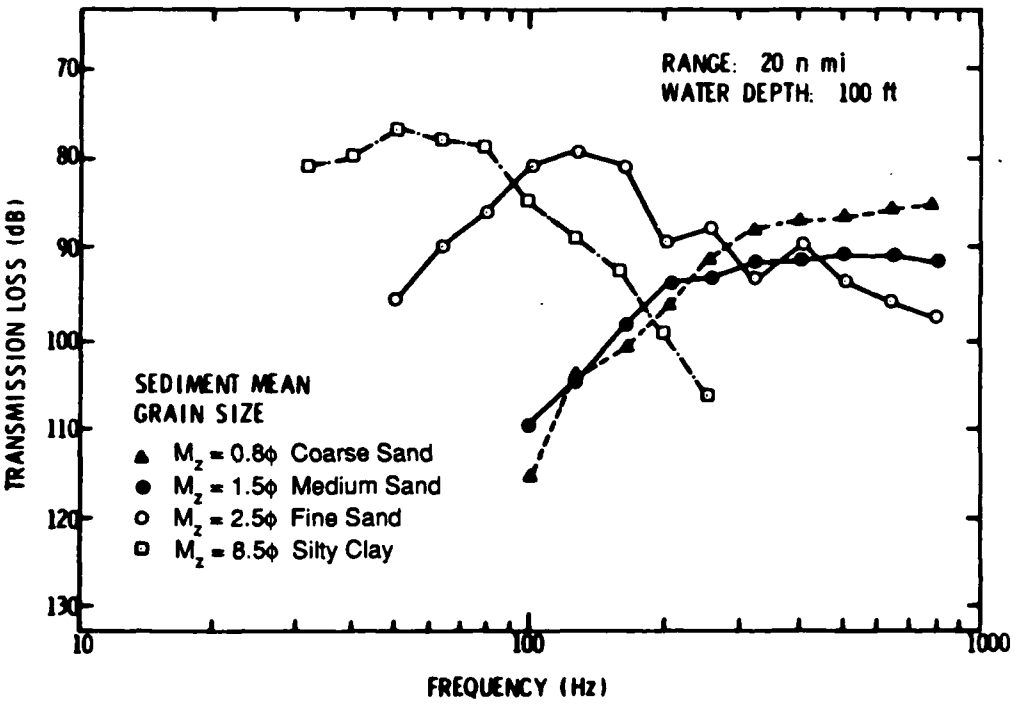

Fig. VI-2. Transmission loss for varied sediment types at a range of 20 nautical miles. (Ref. 31)

cannot be attributed to shear wave generation, since measurements of near surface shear wave velocities at the medium sand site (ϕ = 1.5) yielded V_s < 200 m/s. This is insufficient to account for the observed results.

3. Frequency Dependence of the Compressional Wave Attenuation Rate

McDaniel and Beebe found further that the sediment attenuation rate followed a frequency law like

$$a_p = Af^n \quad \text{dB/km} \ ,$$

where A and n are constants, and the value of n is between 1 and 1.8. The sediment absorption rate is shown in Figure VI-3 as a function of mean grain size, M_z in ϕ-units. For the finer sediments, n=1 and the results agree with those of Hamilton.[64]

4. Shear Wave Loss

Jensen and Kuperman[27] found an optimum frequency of about 250 Hz for propagation over a homogeneous sand bottom during the summer in coastal areas of the eastern North Atlantic. The water depth was about 120 m. They found that normal mode calculations could be brought into agreement with measurements by including rigidity and the effects of shear wave generation, as shown in Figure VI-4. The figure shows that, for a 100 m water layer, the shear wave contribution becomes important when the

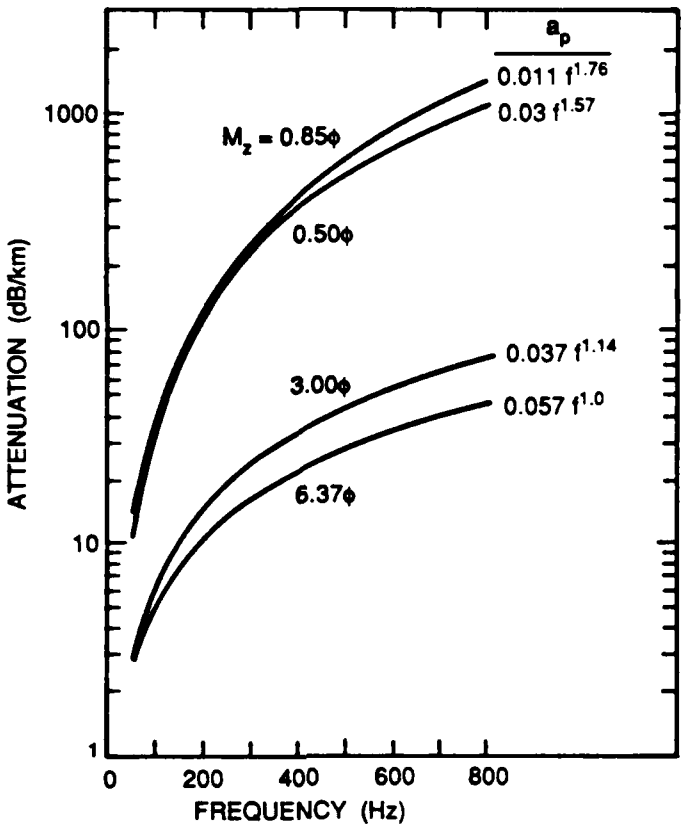

Fig. VI-3. Predicted sediment absorption. (Ref. 37)

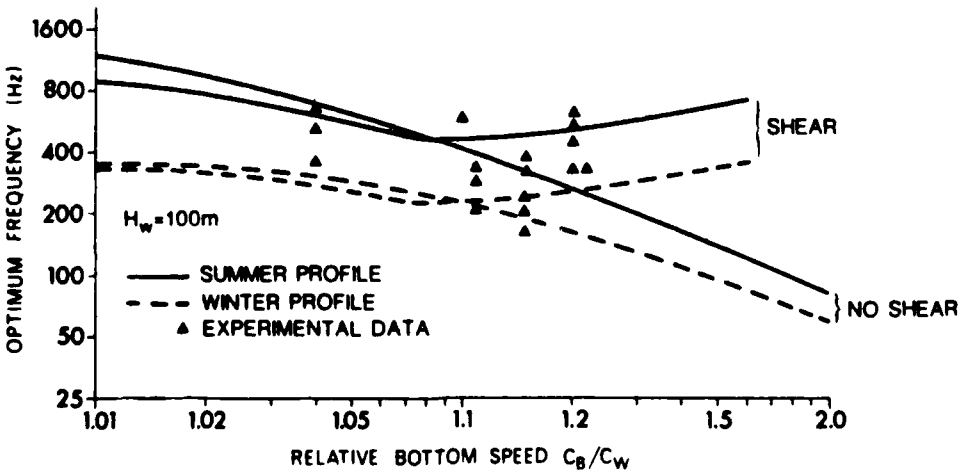

Fig. VI-4. Optimum frequency versus relative bottom speed for a water depth of 100 m. The experimental data are compared with normal-mode theory computations. (Ref. 27)

ratio of the bottom to water compressional wave speed is greater than about 1.2. They show in Table VI-1 that this requires a sediment shear velocity of 600 m/s and a density relative to water of 2, which corresponds to coarse sand. For their calculations they assume that the sediment loss rate for compressional waves is proportional to frequency.

In expanding on the important role that shear wave generation plays in viscoelastic bottom materials, Akal and Jensen[28] start with the sand bottom model shown in Figure VI-5. They show that when the effect of shear is introduced the computed transmission loss at a range of 30 km can be brought into line with measurements (see Figure VI-6).

They claim that a lossy seabed causes attenuation from both compressional wave attenuation in the bottom and the coupling of sound into shear waves. The frequency dependent effect of the seabed on propagation is such that bottom loss increases with decreasing frequency down to near the cutoff (~10 Hz in this case) where interface waves

Table VI-1. Geoacoustic parameters for different bottom types. In the present text, β_c, compressional attenuation, is $a_{p\lambda}$; β_s, shear attenuation, is $a_{s\lambda}$. (Ref. 27)

Bottom type	Porosity P(%)	Relative density ρ_b/ρ_w	Relative speed C_b/C_w	Compressional speed C_b(m/s)*	Shear speed C_s(m/s)	Compressional attenuation β_c(dB/λ)	Shear attenuation β_s(dB/λ)
Clay–silt	60	1.6	1.01	1515	100	0.5	1.0
Sand–silt–clay	55	1.7	1.02	1530	150	0.8	1.5
Silt	50	1.8	1.05	1575 (1600)	200	1.0	2.0
Sand–silt	40	1.9	1.1	1650	400	0.8	1.5
Coarse sand	35	2.0	1.2	1800	600	0.7	1.5
Chalk–limestone	···	2.2	1.5	2250	1000	0.4	1.0
Limestone	···	2.4	2.0	3000	1500	0.3	0.5
Basalt	···	2.6	3.5	5250	2500	0.2	0.5

*C_w = 1500 m/s.

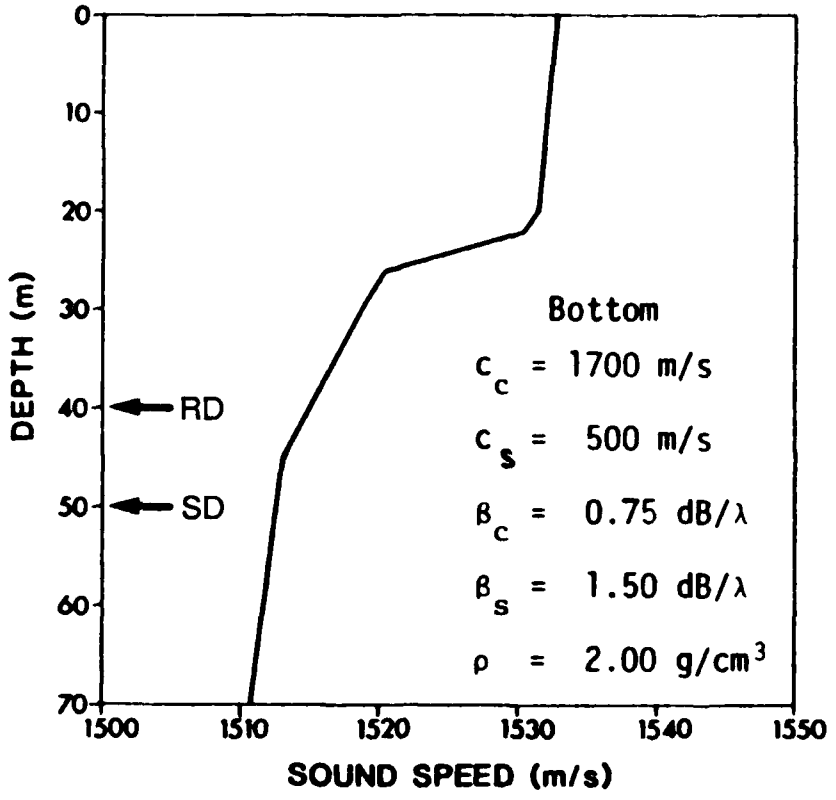

Fig. VI-5. Sound-speed profile and bottom parameters for shallow-water area in southern Mediterranean. In the present text, $\beta_c = a_{p\lambda}$ and $\beta_s = a_{s\lambda}$ (Ref. 28)

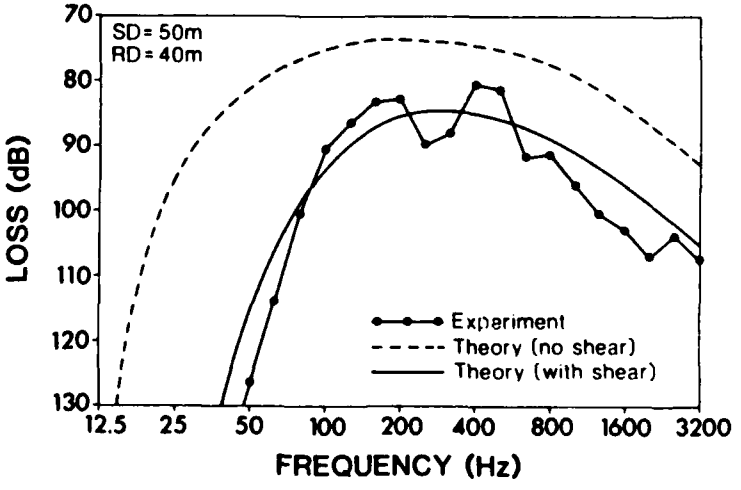

Fig. VI-6. Measured and computed propagation losses at range 30 km. (Ref. 28)

on the seafloor become important propagation paths. Also, they find that propagation levels in the water column are strongly dependent on the bottom type, but that the optimum frequency in the water column is only slightly dependent on seabed properties. They support their claim with broadband propagation data that were collected in different areas of the Mediterranean Sea and eastern North Atlantic. They assume viscoelastic sediments and show that the neglect of shear wave coupling is justified only for very soft sediments like clayey-silts, where the shear wave velocity is very low (<200 m/s).

Their calculations are summarized in Figure VI-7. It is surprising that above 20 Hz a silt bottom shows less transmission loss than sand or limestone. This is apparently due to the lack of excitation of lossy interface waves which would be more prominent in sediments with higher shear speeds.

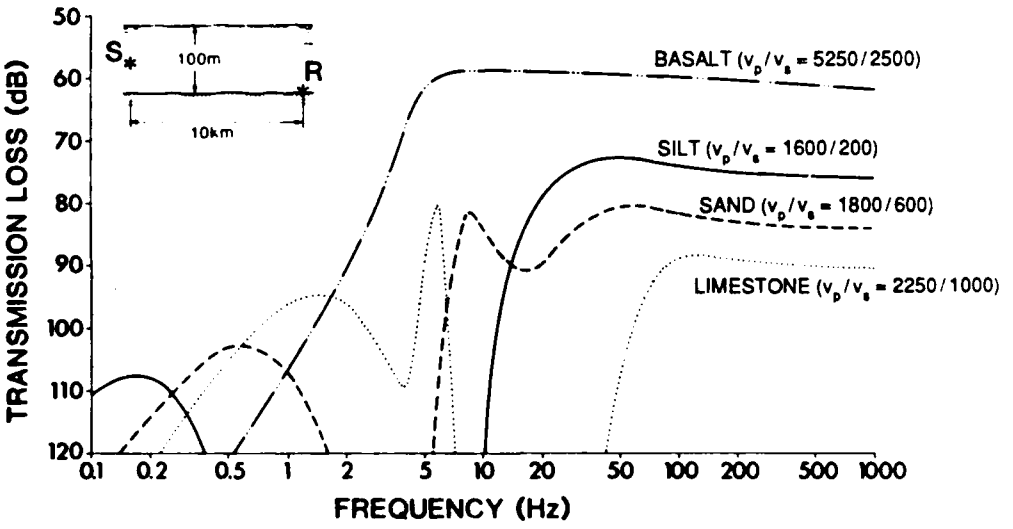

Fig. VI-7 Broadband propagation characteristics for different bottom types. Numbers in parentheses are compressional and shear speeds, respectively. (Ref. 28)

AD-A173 885 LOW-FREQUENCY SHALLOW WATER ACOUSTICS (20 TO 500 HZ) 2/2
(U) WASHINGTON UNIV SEATTLE APPLIED PHYSICS LAB
M SCHULKIN ET AL MAY 86 APL-UW-8606 N00014-84-K-0646
UNCLASSIFIED F/G 20/1 NL

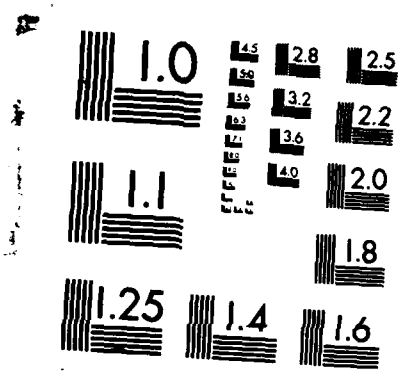

Using Biot poroviscoelastic theory, Yamamoto[11] finds that losses owing to generation of shear waves are unimportant for shear wave velocities less than 550 m/s. In a later study, Eller and Gershfeld[65] used viscoelastic theory to compare the effect of varying shear wave velocity on the angular loss rate as a function of sediment type. They find that the angular loss rate increases sharply in sands for shear wave speeds above about 400 m/s.

On the other hand, Brocher *et al.*[47] found that for frequencies of 5 to 40 Hz, over a shallow sandy bottom off Nova Scotia, nearly all the loss was due to sediment compressional wave attenuation and not the result of conversion to shear waves or interface waves. Furthermore, beyond a certain range, signals below the nominal cutoff frequency differed only slightly from those above the nominal cutoff. He also reported a strong azimuthal dependence.

Lindop[66] and Harrison and Cousins[67] have used propagation loss data, along with a three-layer water-sediment-bedrock model, to deduce the thickness of sediments over the propagation path. The runs were made at low frequency (25 to 500 Hz) in a water depth of 200 m. They found that the optimum frequency depended on the sediment thickness and type. They started with the theoretical concept that the generation of downward propagating shear waves is the main cause of loss for a thin layer or no layer of sediment over bedrock. Because of the screening of the bedrock there is a decreasing loss as the

thickness of a low loss sediment layer increases to tens of meters. On the other hand, there is an increasing loss with sediment thickness if the sediment is very lossy.

Lindop's findings agree with measurements by Weston[68] in the Central North Sea. Weston found an optimum frequency of 200 Hz over a sand bottom in about 75 m of water. High loss areas were found to have an exposed rock bottom or a thin sediment cover. Low loss areas were associated with a thick sediment layer of mud. Optimal frequencies were typically one octave greater in high loss areas than in low loss areas.

Kibblewhite and Denham[69,70] made measurements in the winter and summer over a path off the west coast of New Zealand. The path had a flat thick layer of unconsolidated sediment in 75 m of water. In the winter, four of five tracks had a minimum attenuation rate at 50 to 150 Hz. The one anomalous case showed a monotonic decreasing loss rate with decreasing frequency owing to effects of sediment layering and deep refraction paths in the bottom. In the summer, three of the five tracks showed a minimum loss band and attenuation rates that were higher than those in the winter.

5. Low-frequency Response of Shallow Water Ducts

Eller and Gershfeld[65] treat two canonical models of bottom structure: (1) an isovelocity fast sediment, typically sand which has a sound speed substantially greater than that of water (Pekeris model), and (2) a slow sediment whose sound speed at the interface equals that of the water and which has a positive upward refracting gradient. Each of

these models gives rise to an optimal frequency with least attenuation rate. Model 2 also predicts attenuation rates that decrease with decreasing frequency in a region below about 25 Hz.

For Model 1, acoustic energy is returned from the bottom primarily by reflections at the water-sediment interface. However, there should be an angle of high loss where shear waves are being set up. At low frequencies, mode steepening related to the need to satisfy phase relationships causes modal attenuation to increase with decreasing frequency. There is also an increasing loss from seawater absorption at higher frequencies. The resulting minimum attenuation occurs at a frequency given by

$$f_{min} = 184\,(bC_1^2/H^3)^{1/4} \quad \text{hertz}$$

where

H = water depth, m
C_1 = sound speed, in m/s
b = attenuation rate in dB/radian.

For Model 2, typically mud, the sediment velocity has a positive gradient whose value at the interface equals the sound speed of the water. Acoustic energy is returned to the water column primarily by upward refraction within the sediment. There is again a fre-

quency of minimum attenuation rate. However, there is also a frequency of maximum attenuation rate, which for the first mode is given by

$$f_{max} = 3/8\,(C_1^3/gH^3)^{1/2} \quad \text{hertz}$$

where

g = the sound speed gradient, s^{-1}.

Below f_{max} the attenuation decreases with decreasing frequency. At these low frequencies the ocean bottom ceases to confine the acoustic field as a waveguide. The field extends deeper into the bottom and takes advantage of the decreased sediment absorption at low frequency.

Modal attenuation rates in the second model are very sensitive to slight departures from unity of the sound-speed ratio at the water-sediment interface. For a sediment whose sound speed is slightly less than that of water, one finds the formation of relatively narrow frequency passbands centered approximately at

$$f_{min} = \begin{matrix} 1.1g & \left[1-(C_2/C_1)^2\right]^{-3/2}, \\ 2.6g & \left[1-(C_2/C_1)^2\right]^{-3/2}, \\ & \ldots \qquad . \end{matrix} \quad \text{hertz}$$

Outside of these passbands, substantial rejection bands occur where the acoustic losses are exceptionally high.

VII. SUMMARY AND CONCLUSIONS

The most important requirement for the understanding and prediction of low-frequency, shallow-water acoustic propagation is a knowledge of the geoacoustic parameters and their layered distribution in depth (geoacoustic model). We have considered only the case of lateral uniformity.

In the frequency range 20 to 500 Hz, Biot theory should be applied wherever possible in the calculation of acoustic behavior. Important differences arise at small grazing angles from calculations using viscoelastic models.

In situ methods of measurement of Biot parameters should be continued and improved. The most important Biot parameters are permeability, skeletal frame loss, and complex shear modulus. Wherever the consequences of the Biot acoustic theory of saturated sediments differ from those of viscoelastic theory, the sediment relaxation frequency, f_r, must be determined:

$$f_r = \frac{\beta\eta}{3\pi B} .$$

In this equation, β is the porosity, η is the kinematic viscosity, and B is the specific permeability. At present, the permeability is estimated from mean grain size using the McDaniel-Beebe relationship or the Hazen formula. Since there is a large vertical anisotropy in permeability, it is important to measure its depth dependence as well.

Owing to the relaxation process, the sound wave is dispersive, and a measurement of its velocity at the relaxation frequency yields the sediment porosity. A velocity measurement at very low frequency will then yield the permeability.

The shear modulus of the frame and the frame loss are next in importance. The shear modulus profile can be determined *in situ* in at least two ways. Yamamoto has shown how to estimate the shear profile from motion in the seabed induced by surface gravity waves. Water-seabed interface waves (Stoneley) can also be used to estimate the shear profile.

Attention must be given to the specification of geoacoustic models. A geoacoustic model is used for the solution of the wave equation in layered media along with appropriate boundary conditions. It must have a resolution of detail consistent with the acoustic wavelength under study. For example, Matthews *et al.* and Rubano have arrived at two quite different geoacoustic models for the same Corpus Christi site. While seasonal changes have accounted for some discrepancy, the sound speed values, the depth extent of silty clay and sand layers, and the attenuation for each sediment type are quite different for the two models.

REFERENCES

1. R.K. Matthews, *Dynamic Stratigraphy: An Introduction to Sedimentation and Stratigraphy* (Prentice-Hall, Englewood Cliffs, N.J., 1984), 512 pp.

2. H.J. McLellan, *Elements of Physical Oceanography,* (Pergamon Press, New York, 1977), p.5.

3. *The Application of Oceanography to Subsurface Warfare,* J.T. Tate, U.S. Department of Commerce, AD 200784, 1946, pp. 91-99.

4. C.L. Pekeris, "Theory of propagation of explosive sound in shallow water," in *Propagation of Sound in the Ocean,* M. Ewing, J.L. Worzel, and C.L. Pekeris (The Geological Society of America, Memoir 27, Boulder, Colorado, 1948).

5. K.V. Mackenzie, "Reflection of sound from coastal bottoms," J. Acoust. Soc. Am., **32**, 221-231 (1980).

6. L.M. Brekhovskikh, *Waves in Layered Media* (Academic Press, New York, 1960), Chapter V: "Wave propagation in layers; Chapter VI: "The field of a concentrated source in a layered-inhomogeneous medium."

7. R.D. Stoll and G.M. Bryan, "Wave attenuation in saturated sediments," J. Acoust. Soc. Am. **47**, 1440-1447 (1970).

8. M.A. Biot, "Theory of elastic waves in a fluid-saturated porous solid. I. Low frequency range," J. Acoust. Soc. Am. **28**, 168-178 (1956).

9. M.A. Biot, "Theory of elastic waves in a fluid-saturated porous solid. II. Higher frequency range," J. Acoust. Soc. Am. **28**, 179-191 (1956).

10. M.A.Biot, "Mechanics of deformation and acoustic propagation in porous media," J. Appl. Phys. **33**, 1482-1498 (1962).

11. T. Yamamoto, "Acoustic propagation in the ocean with a poro-elastic bottom," J. Acoust. Soc. Am. **73**, 1587-1596 (1983).

12. H.P. Bucker, J.A. Whitney, and D.L. Keir, "Use of Stoneley waves to determine the shear velocity in ocean sediments," J. Acoust. Soc. Am. **36**, 1595-1596 (1964).

13. T. Yamamoto and T. Torii, "Seabed shear modulus profile inversion using surface gravity (water) wave induced bottom motion," Geophys. J. R. Astr. Soc. **85**, 413-431 (1986).

14. F.P. Shepard, "Nomenclature based on sand-silt-clay ratios," J. Sedimentary Petrology **24**, 151-158 (1954).

15. E.L. Hamilton, unpublished manuscript.

16. E.L. Hamilton, "Geoacoustic modeling of the sea floor," J. Acoust. Soc. Am. **68**, 1313-1340 (1980).

17. E.L. Hamilton, "Sound velocity-density relations in sea-floor sediments and rocks," J. Acoust. Soc. Am. **63**, 366-377 (1978).

18. E.L. Hamilton, "Sound attenuation as a function of depth in the sea floor," J. Acoust. Soc. Am. **59**, 528-535 (1976).

19. Y. Ohta and N. Goto, "Empirical shear wave velocity equations in terms of characteristic soil indexes," Earthquake Engineering and Structural Dynamics, **6**, 167-187 (1978).

20. E.L. Hamilton, "Compressional-wave attenuation in marine sediments," Geophysics, **37**, 620-646 (1972).

21. R.D. Stoll, "Acoustic waves in saturated sediments" in *Physics of Sound in Marine Sediments*, L. Hampton, Ed. (Plenum Press, New York, 1974), pp. 19-39.

22. R.D. Stoll, "Experimental studies of attenuation in sediments," J. Acoust. Soc. Am. **66**, 1152-1160 (1979).

23. J.M. Hovem, "The nonlinearity parameter of saturated marine sediments," J. Acoust. Soc. Am. **66**, 1463-1467 (1979).

24. J.M. Hovem and G.D. Ingram, "Viscous attenuation of sound in saturated sand," J. Acoust. Soc. Am. **66**, 1807-1812 (1979).

25. Yu. P. Neprochnov, "Seismic studies of the crustal structure beneath the seas and oceans," Oceanology **11**, 709-715 (1971) (Translation).

26. S.K. Mitchell and K.C. Focke, "The role of the seabottom attenuation profile in shallow water acoustic propagation," ARL-TP-82-27, Applied Research Laboratories, University of Texas, 1982.

27. F.B. Jensen and W.A. Kuperman, "Optimum frequency of propagation in shallow water environments," J. Acoust. Soc. Am. **73**, 813-819 (1983).

28. T. Akal and F.B. Jensen, "Effects of the sea-bed on acoustic propagation" in *Acoustics and the Sea-Bed: Conference Proceedings*, N.G. Pace, Ed. (Bath University Press, Bath, UK, 1983), pp. 225-232.

29. R.H. Bennett, NORDA Technical Note 318, July 1985, p. 13f; personal communication re in-situ geotechnical probes.

30. J.E. Matthews, "Shear wave velocity measurements in marine sediments," Geo-Marine Letters **2**, 215-217 (1982).

31. S.T. McDaniel and J.H. Beebe, "Semi-empirical sea-bed models based on Biot theory," in *Acoustics and the Sea-Bed*, N.G. Pace, Ed. (Bath University Press, Bath, UK, 1983) pp. 63-70.

32. W.C. Krumbein and G.D. Monk, "Permeability as a function of the size parameters of unconsolidated sand," Tech. Pub. No. 1492, Petr. Technol., Am. Inst. Mining and Metall. Eng., **5**, 1-11 (1942).

33. P.C. Carman, *Flow of Gases through Porous Media* (Academic Press, New York, 1956).

34. T.W. Lambe and R.V. Whitman, *Soil Mechanics* (John Wiley & Sons, New York, 1969), p. 287.

35. T. Yamamoto and R.H. Bennett, "Laboratory measurements of selected geo-acoustic properties of carbonate sediments at the Great Bahama Bank," presented at the 111^{th} meeting of the ASA, May 1986 (abs. J. Acoust. Soc. Am. **79**, Suppl.1, paper T7, 1986).

36. R.D. Stoll, "Marine sediment acoustics," J. Acoust. Soc. Am. **77**, 1789-1799 (1985).

37. J.H. Beebe, S.T. McDaniel, and L.A. Rubano, "Shallow-water transmission loss prediction using the Biot sediment model," J. Acoust. Soc. Am. **71**, 1417-1426 (1982).

38. J.F. Miller and S.N. Wolf, "Model acoustic transmission loss (MOATL): A transmission-loss computer program using a normal-mode model of the acoustic field in the ocean," NRL Report No. 8429, Naval Research Laboratory, Washington, D.C., 1980.

39. H.W. Kutschale, "Rapid computation by wave theory of propagation loss in the Arctic Ocean," Technical Report No. 8, Lamont-Doherty Geological Observatory of Columbia University, Palisades, NY, March 1973.

40. S.T. McDaniel, "Parabolic approximations to underwater sound propagation," J. Acoust. Soc. Am. **58**, 1178-1185 (1975).

41. I. Tolstoy, "Shallow water test of the theory of layered wave guides," J. Acoust. Soc. Am. **30**, 348-361 (1958).

42. J.E. Matthews, P. Bucca, and W.Geddes, "Preliminary environmental assessment of the PROJECT GEMINI site, Corpus Christi, Texas," NORDA Report No. 120, Naval Ocean Research and Development Activity, NSTL, MS, June 1985.

43. L.A. Rubano, "Acoustic propagation in shallow water over a low-velocity bottom," J. Acoust. Soc. Am. **67**, 1608-1613 (1980).

44. F.B. Jensen and M.C. Ferla, "SNAP: The SACLANTCEN Normal-Mode Acoustic Propagation Model," SACLANCENTEN SM-121, SACLANT ASW Research Centre, La Spezia, Italy, 1979, pp. 1-92.

45. S.T. McDaniel and J.H. Beebe, "Influence of semi-consolidated sediments on sound propagation in a coastal region" in *Bottom-Interacting Ocean Acoustics*, W.A. Kuperman and F.B. Jensen, Eds. (Plenum Press, New York, 1980), pp. 493-505.

46. I. Tolstoy, "Guided waves in a fluid with continuously variable velocity overlying an elastic solid: Theory and experiment," J. Acoust. Soc. Am. **32**, 81-87 (1960).

47. T.M. Brocher, B.T. Iwatake, and D.A. Lindwall, "Experimental studies of low-frequency waterborne and sediment-borne acoustic wave propagation on a continental shelf," J. Acoust. Soc. Am. **74**, 960-972 (1983).

48. M. Schulkin and W.H. Thorp, "Study D: Transmission by way of the bottom," in USL Research Report No. 255, Report on the Status of Project AMOS (Acoustic, Meteorological, and Oceanographic Survey), by H.W. Marsh and M. Schulkin, 21 March 1955, pp. 33-39.

49. O.F. Hastrup, "Some bottom-reflection loss anomalies near grazing and their effect on propagation in shallow water," in *Bottom-Interacting Ocean Acoustics*, W.A. Kuperman and F.B. Jensen, Eds. (Plenum Press, New York, 1980), pp. 135-152.

50. E. Strick and A.G. Ginzbarg, "Stoneley wave velocities for a fluid-solid interface," Bull. Seismol. Soc. Am. **46**, 281-292 (1956).

51. S.R. Rutherford and K.E. Hawker, "The effects of density gradients on bottom reflection loss for a class of marine sediments," J. Acoust. Soc. Am. **63**, 750-757 (1978).

52. K.E. Hawker, W.E. Williams, and T.L. Foreman, "A study of the acoustical effects of sub-bottom absorption profiles," J. Acoust. Soc. Am. **65**, 360-367 (1979).

53. K.E. Hawker, "The influence of Stoneley waves on plane wave reflection coefficients: Characteristics of bottom reflection loss," J. Acoust. Soc. Am **64**, 548-555 (1978).

54. K.E. Hawker, "The existence of Stoneley waves as a loss mechanism in plane wave reflection problems," J. Acoust. Soc. Am. **65**, 682-686 (1979).

55. K.E. Hawker and T.L. Foreman, "A plane wave reflection loss model based on numerical integration," J. Acoust. Soc. Am. **64**, 1470-1477 (1978).

56. G.J. Fryer, "Reflectivity of the ocean bottom at low frequency," J. Acoust. Soc. Am. **63**, 35-42 (1978).

57. W.T. Thomson, "Transmission of elastic waves through a stratified solid medium," J. Appl. Phys. **21**, 89-93 (1950).

58. N.A. Haskell, "The dispersion of surface waves on multilayered media," Bull. Seismol. Soc. Am. **43**, 17-34 (1953).

59. P.J. Vidmar and T.L. Foreman, "A plane-wave reflection loss model including sediment rigidity," J. Acoust. Soc. Am. **66**, 1830-1835 (1979).

60. F. Gilbert and G.E. Backus, "Propagator matrices in elastic wave and vibration problems," Geophysics **31**, 326-332 (1966).

61. R.D. Stoll and T.-K. Kan, "Reflection of acoustic waves at a water-sediment interface," J. Acoust. Soc. Am. **70**, 149-156 (1981).

62. R.D. Stoll, "Acoustic waves in ocean sediments," Geophysics **42**, 715-725 (1977).

63. T. Akal, "Sea floor effects on shallow-water acoustic propagation," in *Bottom-Interacting Ocean Acoustics*, W.P. Kuperman and F.B. Jensen, Eds. (Plenum Press, New York, 1980) pp. 557-575.

64. E.L. Hamilton, "Sound attenuation in marine sediments," NUCTP 281 Naval Undersea Research and Development Center, San Diego, California, 1972.

65. A.I. Eller and D.A. Gershfeld, "Low-frequency acoustic response of shallow water ducts," J. Acoust. Soc. Am. **78**, 622-631 (1985).

66. P.H. Lindop, "The deduction of approximate values of sediment depth from propagation loss measurements," in *Ocean Seismo-Acoustics — Low Frequency Underwater Acoustics*, T. Akal and J.M. Berkson, Ed., (Plenum Press, New York, 1986).

67. C.H. Harrison and P.L. Cousins, "A study of propagation loss dependence on sediment layer thickness using the fast field program," in *Ocean Seismo-Acoustics — Low Frequency Underwater Acoustics*, T. Akal and J.M. Berkson, Ed., (Plenum Press, New York, 1986).

68. D.E. Weston, "Propagation of sound in shallow water," J. Br. IRE **26**, 329-337 (1963).

69. A.C. Kibblewhite and R.N. Denham, "Experiment on sound propagation in shallow water under isovelocity conditions," J. Acoust. Soc. Am. **40**, 1337-1344 (1966).

70. A.C. Kibblewhite and R.N. Denham, "Experiment on sound propagation in shallow water with velocity structure," J. Acoust. Soc. Am. **44**, 104-112 (1968).

UNCLASSIFIED

SECURITY CLASSIFICATION OF THIS PAGE (When Data Entered)

REPORT DOCUMENTATION PAGE		READ INSTRUCTIONS BEFORE COMPLETING FORM
1. REPORT NUMBER APL-UW 8606	2. GOVT ACCESSION NO. ADA173885	3. RECIPIENT'S CATALOG NUMBER
4. TITLE (and Subtitle) Low-Frequency Shallow Water Acoustics (20 to 500 Hz)		5. TYPE OF REPORT & PERIOD COVERED
		6. PERFORMING ORG. REPORT NUMBER APL-UW 8606
7. AUTHOR(s) M. Schulkin J.A. Mercer		8. CONTRACT OR GRANT NUMBER(s) N00014-84-K-0646 Mod 1
9. PERFORMING ORGANIZATION NAME AND ADDRESS Applied Physics Laboratory University of Washington 1013 NE 40th Street Seattle, Washington 98105		10. PROGRAM ELEMENT, PROJECT, TASK AREA & WORK UNIT NUMBERS
11. CONTROLLING OFFICE NAME AND ADDRESS Office of Naval Research (Code 425UA) 800 N. Quincy Street Arlington, VA 22217		12. REPORT DATE May 1986 13. NUMBER OF PAGES 111
14. MONITORING AGENCY NAME & ADDRESS(if different from Controlling Office)		15. SECURITY CLASS. (of this report) UNCLASSIFIED 15a. DECLASSIFICATION DOWNGRADING SCHEDULE

16. DISTRIBUTION STATEMENT (of this Report)

Approved for public release; distribution unlimited.

17. DISTRIBUTION STATEMENT (of the abstract entered in Block 20, if different from Report)

18. SUPPLEMENTARY NOTES

19. KEY WORDS (Continue on reverse side if necessary and identify by block number)

Biot theory	permeability	viscoelastic models
complex shear modulus	porosity	skeletal frame loss
compressional wave	shear wave	
dispersion	sediment relaxation frequency	
geoacoustic parameters	low-frequency, shallow-water acoustic propagation	

20. ABSTRACT (Continue on reverse side if necessary and identify by block number)

The parameters affecting shallow water acoustic behavior at low frequencies (20 to 500 Hz) have been reviewed. ~~and an assessment~~ has been made of their relative ~~importance~~. The depth dependence of the sediment parameters, and stratigraphic layering in depth, form the basis of geoacoustic models for which the wave equation may be solved. ~~It is found that~~ there is no unique approach to geoacoustic modeling. Typically, the additional information required includes *in situ* refraction, dispersion, and reflection measurements. Application of the Biot theory of sediment acoustics, which uses poroviscous para-

DD FORM 1 JAN 73 1473 EDITION OF 1 NOV 65 IS OBSOLETE
S/N 0102-LF-014-6601

UNCLASSIFIED

SECURITY CLASSIFICATION OF THIS PAGE (When Data Entered)

20. ABSTRACT, Cont'd.

meters, leads to different conclusions in the frequency range of interest from those calculated using standard viscoelastic parameters alone. The Biot acoustic theory also explains successful data fits to semiempirical compressional and shear wave results. The most important sediment property is the flow permeability, which is equal to the choice of acoustic frequency in its effect. Its range of variability is so large that it is necessary to make a specific *in situ* determination of its magnitude for use in modeling and prediction. The permeability controls the relaxation frequency of the sediment and thus the rate of attenuation of both compressional and shear waves, their frequency dependence, and their velocity dispersion. Next in importance ~~and requiring similar attention~~ are the shear properties of the sediments, their related interface waves, and the skeletal frame loss. It is ~~concluded~~ that determination of these parameters *in situ* and further study in the laboratory are most important for progress.

END

12-86

DTIC